Centre for Geo-Information

Thesis report GIRS-2015-32

Characterizing small green landscape elements from airborne LiDAR data

minor thesis

Annemieke de Kort

20-08-2015

WAGENINGEN UNIVERSITY
WAGENINGEN UR

Picture front page: Still of drone video of Het Curringherveld in Het Zuidelijk Westerkwartier in Groningen, taken at 25.06.2014 (source: www.cenhek.nl/G0251343.JPG)

Characterizing small green landscape elements from airborne LiDAR data

minor thesis

Annemieke de Kort

Registration number 710610-468-100

Supervisors:

Harm Bartholomeus

Frans Rip

20-08-2015

Wageningen, The Netherlands

Thesis code number: GRS-80418

Wageningen University and Research Centre
Laboratory of Geo-Information Science and Remote Sensing

Abstract

Degradation of small green landscape elements is an occurring problem in the Netherlands. To tackle the problem, a new management system to restore nature is in development. In this thesis research, a data processing model was developed to support the new management system. The model, that uses AHN2 point cloud LiDAR data to classify small green landscape elements, was built up in two steps. In the first step, a vegetation dataset was created from the AHN2 dataset. In the second step, small green landscape elements were classified from the vegetation dataset. The development of the model was based on statistical analysis: statistics were calculated and analysed for different small green landscape elements and used as selection criteria in the model. LAStools, in combination with ArcGIS was used to create the model. Although no problems occurred during the first step, the second step resulted in poor classification. From the 17 small green landscape elements that were available for validation, 10 elements were not classified at all, whereas from the other elements, only two small green landscape elements were classified correctly. Poor classification results are likely caused by the small sample size that was available during this thesis research. It is therefore recommended to calibrate and validate the data processing model in another area where sufficient amounts of samples for calibration and validation can be collected, and to add other selection criteria to the model, to increase classification results and make the model a useful element in the new management system.

Keywords: *small green landscape elements, point cloud LiDAR, AHN2, statistical analysis, LAStools, ArcGIS*

Table of contents

List of Figures

List of Tables

1 Introduction

Degradation of small green landscape elements and a decrease in species that depend on them is an occurring problem in the Netherlands. When too many species disappear, the Netherlands cannot longer satisfy international demands for the protection of species. A new nature management system to restore nature is therefore in development. In this thesis research, it is examined if a data processing model for small green landscape element detection from airborne LiDAR data can be developed to support the new nature management system. With such a model, subsidy applications can be dealt with easier and faster, improving the efficiency of the system.

Chapter 1 provides background information about the new nature management system and the basic principles of airborne LiDAR. Furthermore, the problem definition, research objective and research questions of this thesis research are defined and the outline of this report is given.

1.1 The Agricultural Nature and Landscape Management System

In 2016, a new agricultural and nature management system, the Agricultural Nature and Landscape Management (Agrarisch Natuur- en Landschapsbeheer, ANLb) system, will be implemented in the Netherlands. The new system is an improvement of the current system, the Subsidy System Nature and Landscape (Subsidiestelsel Natuur en Landschap, SNL), that is found to be too inefficient and too expensive (Hammers *et al*., 2014; Melman *et al*., 2014; Mulders, 2014). The ANLb system needs to contribute to a countryside that is attractive and liveable for both humans and animals. Moreover, the ANLb system needs to satisfy international obligations of the Netherlands towards the Bird and Habitat Directive (Vogel- en Habitatrichtlijn, VHR) and the Framework Directive Water (Kaderrichtlijn Water, KRW), as defined by the European Union (Mulders, 2014).

To satisfy the VHR and the KRW, specialists have carried out an inventory of in the Netherlands occurring endangered species. Based on this inventory, descriptions of various agricultural landscapes that have potential for the survival of these species were made by the Governmental Service for Land and Water Management (Dienst Landelijk Gebied, DLG) and research institute Alterra (Hammers *et al*., 2014). Potential agricultural landscapes range from large scale open areas with grasslands or arable lands to small scale closed areas with a large variation in green and blue landscape elements (Hammers *et al*., 2014). Integrating these agricultural landscapes in existing agricultural areas will make these areas better suitable for endangered species and will therefore increase their chances to survive.

A subsidy application system to support the ANLb system is currently in development. With the help of this system, agricultural collectives, existing of various stakeholders in the field of nature and

agriculture, can apply for subsidies to implement measures that are needed to establish new agricultural landscapes or to maintain and improve existing agricultural landscapes in their plan areas. In support of the subsidy application system, information is needed about occurrence, distribution and density of flora and fauna, occurrence of suitable biotopes, and boundaries of plan areas (Melman *et al*., 2014).

Remote Sensing (RS) techniques can be useful to support the subsidy application system, both for the agricultural collectives that apply for the subsidies and for the provinces that need to assess these applications. With the help of RS techniques, it can be determined in a relative easy and fast way where and what kind of measures need to be implemented to make agricultural areas better suitable for endangered species. Integrating RS techniques in the subsidy application system will therefore simplify and accelerate subsidy applications and assessments and improve the efficiency of the system.

1.2 Basic principles of airborne LiDAR

LiDAR (**Li**ght **D**etection **A**nd **R**anging) is an active Remote Sensing technique developed in the 1960s after the invention of laser. Whereas LiDAR was initially used by land surveyors and civil engineers for alignment operations and measurements in tunnels, shafts and on bridges, NASA had started to develop LiDAR techniques for topographic mapping of Artic areas as well (Petrie and Toth, 2009). The introduction of direct geo-referencing technology and the general developments in computer technology in the 1990s gave the use of LiDAR a commercial boost (Petrie and Toth, 2009) and applications evolved from topographic mapping to flood modelling, classification of bare earth ground versus elevated features, vegetation removal, feature extraction and power line modelling (Ussyshkin and Theriault, 2011). In ecology and forestry, LiDAR is used to map ground topography, measure structures and functions of vegetation canopies, and predict forest stand structure attributes such as Leaf Area Index and timber volume (Faridhouseini *et al*., 2011).

LiDAR can be subdivided in space borne LiDAR (when the scanning unit is mounted on a spacecraft), airborne LiDAR (when the scanning unit is mounted on an aircraft) and terrestrial LiDAR (when the scanning unit is ground based). Whereas space borne and airborne LiDAR are able to capture large areas from a top point of view, terrestrial LiDAR is able to capture smaller areas with high accuracy from a side point of view. Terrestrial LiDAR is therefore suitable to reduce uncertainties in calibration and validation data for large scale remote sensing products (Calders, 2015).

Airborne LiDAR systems consist of four major components (Figure 1): a laser emitter-receiver scanning unit, two differential Global Positioning Systems (GPS), one mounted on the aircraft and one ground based, a highly sensitive inertial measurement unit (IMU) attached to the scanning unit, and a computer to control the system and to store the data from the scanner, the two GPS systems and the IMU (Reutebuch *et al*., 2005).

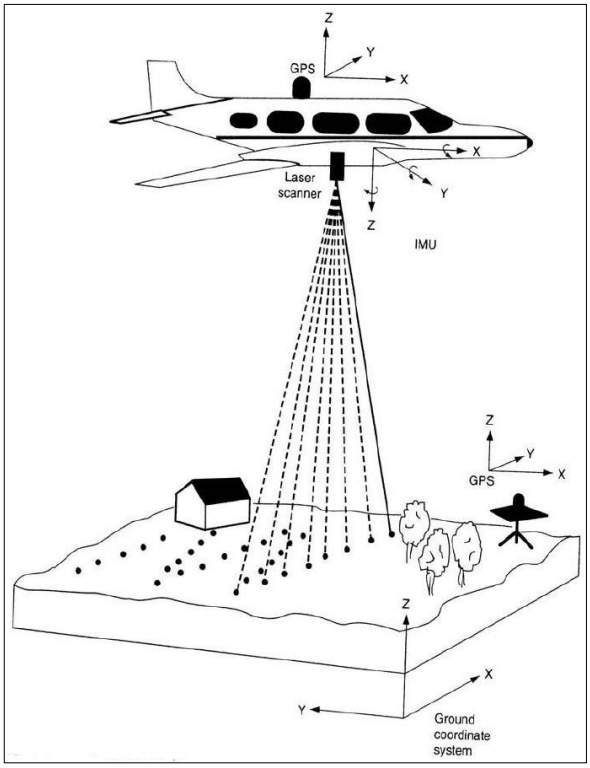

Figure 1: Components of an airborne LiDAR system (source: Lillesand *et al*., 2008)

The laser scanning unit emits near infrared laser pulses to the earth's surface at a high rate and in a consistent pattern within a swath below the aircraft, using an oscillating mirror or a rotating prism, and measures how long it takes for the reflected laser pulses to return to the unit. The two GPS systems and the IMU determine the precise position and attitude of the laser scanner unit with each emitted pulse. The return time for each laser pulse back to the laser scanning unit is processed to calculate the distance between the unit and the various surfaces present on or above the earth's surface (Lillesand *et al*., 2008; Reutebuch *et al*., 2005). The reflected and processed laser pulses from an area are recorded and stored together in a point cloud dataset. By adding a *z*-component to its measurements, LiDAR is able to create 3D visualisations of the landscape (Mücher *et al*., 2014; Faridhouseini *et al*., 2011), making the technique suitable for 3D mapping.

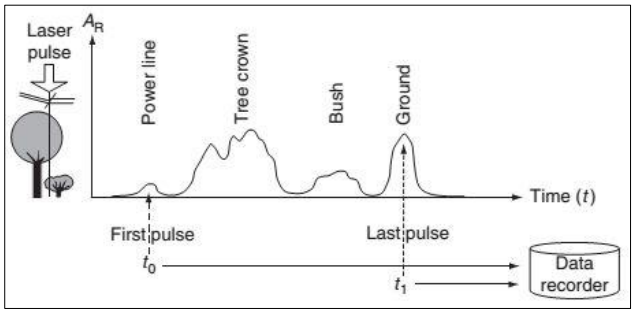

Figure 2: Multiple returns recorded from one emitted laser pulse (source: Petrie and Toth, 2009)

Multiple returns will occur when a laser pulse strikes a target that does not completely block the path of the pulse and the remaining portion of the pulse continues on to a lower object, for example when the pulse reaches a forest canopy that has small gaps between branches and foliage (Reutebuch *et al*., 2005; Figure 2). When only these multiple returns are recorded for each emitted laser pulse, the LiDAR system is categorized as a discrete return (DR) system. However, when the full profile of a return signal is recorded in fixed time intervals, the LiDAR system is categorized as a full waveform (FW) system (Ussyshkin and Theriault, 2011).

LiDAR can be used to collect large amounts of reliable and dense three dimensional point data in a short time span from inaccessible areas, steep slopes, and shadowed areas during day and night and under almost all weather conditions. Accuracy is high and direct and easy acquisition of positional information is possible (Nex and Rinaudo, 2011; Lillesand *et al*., 2008; Petrie and Toth, 2009). The data are georeferenced from the moment they are collected (Lillesand *et al*., 2008) and users do not have to worry about geometric, atmospheric and radiometric corrections (Chen, 2007). Although data acquisition costs were high and processing software was hardly available in the initial phase of LiDAR development, current developments have significantly decreased these acquisition costs and processing software has become available on a commercial base more and more (Chen, 2007; Reutebuch *et al*., 2005).

Although the advantages of LiDAR are numerous, some disadvantages also occur. First of all, LiDAR point cloud datasets often have a large size, not only because of the high amount of laser points that are collected but also because the spatial location of each laser point needs to be explicitly stored (Chen, 2007). Computation time when processing the data might therefore be long. Secondly, information extraction from an unclassified LiDAR point cloud dataset often requires experienced users and complicated software (Nex and Rinaudo, 2011). Thirdly, since many commercial DR systems are focused on topographic two dimensional ground mapping, they often provide a high horizontal ground point density whereas vertical point density is less high. This might limit three dimensional mapping, especially when vegetation canopies need to be analysed. Using data from FW systems can solve this problem, but processing FW data is complex, FW datasets are enormous, and commercial or open source software to process FW data is hardly available (Ussyshkin and Theriault, 2011).

1.3 Problem definition

Small green landscape elements such as trees, hedges and shelterbelts are important elements in the landscape, not only because they improve the visual quality of the landscape, but also because many species depend on these elements for their survival. Small green landscape elements are not only used as shelter, dispersion corridor or forage area (Grashof-Bokdam *et al*., 2009; Geertsema *et al*., 2003), their presence in the landscape also prevents habitats to become disintegrated and isolated from each other and make it possible for species to exchange (Geertsema *et al*., 2003). However, small green landscape elements disappear more and more from the Dutch landscape due to lack of maintenance and developments such as redistribution and scaling up of agricultural areas, agricultural mechanisation and urbanisation (Nieuwenhuizen *et al*., 2008; Koomen *et al*., 2007; Smits and Alebeek, 2007), endangering habitats and therefore the survival of species. To prevent species from extinction, new small green landscape elements need to be constructed and the condition of

existing small green landscape elements needs to be improved. Inventories need to be carried out to determine where and what kind of measures need to be implemented to increase and reinforce the presence of small green landscape elements.

Up to now, vegetation inventories are mainly carried out with the help of topographic maps or land use and land cover (LULC) maps (Ficetola *et al*., 2014; Koomen *et al*., 2007; Geertsema *et al*., 2003), aerial photographs (Mücher *et al*., 2014; Koomen *et al*., 2007) or field work (Mücher *et al*., 2014; Koomen *et al*., 2007). Using these tools, however, has limitations. Topographic maps and LULC maps are often not detailed enough because in many cases they are developed for general purposes only (Ficetola *et al*., 2014; Geertsema *et al*., 2003). Moreover, maps can be unreliable because they are based on human interpretation of aerial photographs and might therefore include human mistakes (Koomen *et al*., 2007). Information about vegetation heights and vegetation types cannot be derived from maps and aerial photographs (Mücher *et al*., 2014; Geertsema *et al*., 2003) but only in the field itself. Field work, however, is labour intensive (Mücher *et al*., 2014) and expensive, especially when large areas need to be explored. To overcome these limitations and improve inventory results, new techniques need to be integrated in inventories.

LiDAR might be a useful technique to support inventories. However, although the use of LiDAR shows an upward trend, not all of its possibilities for vegetation inventories are fully explored yet. Literature research has found that up to now, LiDAR is mainly used for tree inventories in forested or urbanized areas (*e.g*. Liu *et al*., 2013; Ferraz *et al*., 2012) or for vegetation inventories in large areas, such as savannahs, shrub lands and wetlands (*e.g*. Gwenzi and Lefsky, 2014; Ward *et al*., 2013; Estornell *et al*., 2011). The use of LiDAR for small scale vegetation inventories is only found in precision agriculture, where it is used for weed detection in crop fields (Andújar *et al*., 2013; Weiss *et al*., 2010), crop management support (Shafri *et al*., 2012; Willers *et al*., 2012), canopy structure measurement (Weis *et al*., 2013) and individual maize plant detection (Höfle, 2014). In the Netherlands, LiDAR is only used for large scale vegetation inventories, such as floodplain vegetation mapping (Verrelst *et al*., 2009; Geerling *et al*., 2007; Straatsma *et al*., 2004), forest and heathland mapping (Ficetola *et al*., 2014; Mücher *et al*., 2014), detecting tree changes in urban areas (Xiao *et al*., 2012), and invasive woody shrub species mapping in coastal dune landscapes (Hantson *et al*., 2012). No literature was found about the use of LiDAR for the inventory of small green landscape elements, neither in the Netherlands or worldwide, and it is therefore unknown if LiDAR is a suitable technique to detect the presence of small green landscape elements in the landscape.

1.4 Research objective and research questions

The general objective of this thesis research is to examine if unclassified point cloud LiDAR data can be used to create a data processing model that is able to detect small green landscape elements in the Netherlands. Since LiDAR point cloud datasets are often large and computation time can therefore be long, only a small area in the Netherlands is tested. LAStools, in combination with ArcGIS 10.2, and Microsoft Excel 2010 is used for data analysis and to create and validate the model.

To reach the general objective, this research will answer the following research questions:

1. *Which types of small green landscape elements exist in the study area and what are the characteristics of each of these landscape elements?*
2. *Which small green landscape elements can be distinguished from their surrounding environment and from each other when looking at unclassified point cloud LiDAR data only?*
3. *How can automated data processing be helpful in detecting small green landscape elements from unclassified point cloud LiDAR data?*
    a. Can automated data processing be used to distinguish vegetation from its surrounding environment?
    b. Can automated data processing be used to distinguish the different small green landscape elements from each other?

To answer the first research question, a field inventory was carried out to determine which different small green landscape element types are present in the study area, and a statistical analysis of the unclassified point cloud LiDAR dataset was carried out to determine the characteristics of these small green landscape elements. The statistical analysis was carried out with the help of Microsoft Excel 2010. The second research question was answered by carrying out a visual analysis of LiDAR profiles and top views, created in ArcGIS 10.2, of the small green landscape elements that are present in the study area. To answer the third research question and its sub questions, the unclassified point cloud LiDAR dataset and the results of the statistical analysis were used to create and validate a data processing model with the help of LAStools, used in combination with ArcGIS 10.2.

1.5 Thesis outline

This thesis report is structured as follows. In Chapter 2, the methodology that is used for the creation of the data processing model is explained. First, the inventory of the study area and the used data and software are described. Then it is explained how the LiDAR point cloud dataset was pre-processed and visually analysed. Finally, it is explained how the data processing model was created and validated.

In Chapter 3, the results of the data processing modelling are shown and discussed. Chapter 3 starts with a discussion about the inventory of the study area, followed by a discussion about the visual analysis of the LiDAR point cloud dataset. Then, the results of the data processing modelling are shown and discussed. Finally, the validation results are shown and discussed.

In Chapter 4, the final conclusion and recommendations are given.

2 Methodology

In this Chapter, the methodology that is followed in this research is discussed. First, the study area and its inventory is described, after which it is explained what data and software were used to create the data processing model. Then it is explained how the LiDAR point cloud dataset was pre-processed and visually analysed. Finally, it is explained how the data processing model was created and validated. An explanation about the statistical analysis of the LiDAR point cloud dataset is included in the paragraph where the creation of the data processing model is discussed.

2.1 Inventory of the study area

For the purpose of this research, it was important to select a study area that contains different types of small green landscape elements. A few areas in the Netherlands satisfy this demand. One of them is 'Het Zuidelijk Westerkwartier' in the province Groningen. 'Het Zuidelijk Westerkwartier' consists of a small scale closed agricultural landscape where meadows are surrounded by wooded banks, shelterbelts, alder belts and hawthorn hedges. Parts of 'Het Zuidelijk Westerkwartier' are indicated as shelterbelt reserve area where landscape elements need to be maintained and reinforced. The 98 hectare large study area in this research, situated south of the village Kornhorn between 53.1811° and 53.1697° Northern latitude and 6.2336° and 6.2539° Eastern longitude (Figure 3), is one of these reserve areas. The characteristic vegetation in the study area is well preserved and since the study area is not only a reserve area but also belongs to the Ecological Main Structure (Ecologische Hoofdstructuur, EHS), management is aimed at preservation and optimisation of belts, banks and hedges (Natuurbeheerplan Groningen, 2015).

Figure 3: Overview of the study area (source: Google Earth)

To make an inventory of the existing small green landscape elements, the study area was visited twice, on Sunday 8 March 2015 and on Tuesday 24 March 2015. Vegetation was still bare due to the early time of year. Classification of the small green landscape elements was based on the Index Nature and Landscape, a Dutch index where all management types are standardised to make communication between different managers easier (Index Natuur en Landschap, onderdeel Landschapsbeheertypen, version 2015). Personal modifications of the index were sometimes made to make it easier to distinguish the different landscape elements from each other.

Classification was done in the following way (see also the classification tree in Figure 4). All trees and/or shrubs that were situated on a wall of earth were classified as wooded bank. When a group of trees and/or shrubs did not have a linear shape (length >> width) but a polygonal shape (length ≈ width) with a minimal size of two are, it was classified as group of trees. Small green landscape elements with a shrub layer that were not classified as wooded bank or as group of trees were classified as shelterbelt. Small green landscape elements without a shrub layer that were not classified as wooded bank or as group of trees were classified as alder belt when black alder (*Alnus glutinosa)* was the dominating tree type (> 50 per cent occurrence), or as row of trees when black alder was not the dominating tree type (< 50 per cent occurrence).

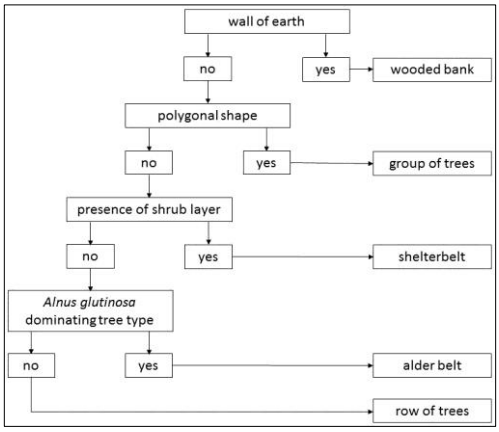

Figure 4: Classification tree of small green landscape elements in the study area

Figure 6: Blume-Leiss inclinometer

To examine if LiDAR point cloud heights did not deviate too much from field heights, heights of some randomly chosen trees and shrubs were measured. Tree and shrub locations were determined with a GPS (type eTrex30, Garmin). Whereas shrub heights could be measured with a measuring tape, tree heights had to be estimated. For this, the distance in meters from the eye level to the stem of the tree was measured with a measuring tape, and the angles in degrees from the eye level to the top and to the bottom of the tree were estimated with a Blume-Leiss inclinometer (Baumhöhenmesser Blume-Leiss, Carl Leiss, Berlin-Steglitz; Figure 6). The tree height was then estimated with the help of the tangent method as explained in Figure 5.

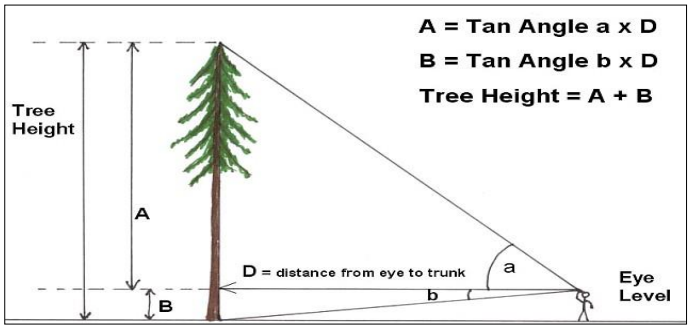

Figure 5: Estimating tree height using the tangent method (source: www.monumentaltrees.com/en/content/measuringheight/)

2.2 Used data and software

To create the data processing model, the Up-to-date Height Model of The Netherlands version 2 (Actueel Hoogtebestand Nederland, AHN2), an airborne point cloud LiDAR dataset that contains detailed height information of the whole country of the Netherlands, was used. The production of the AHN2 dataset was commissioned by Rijkswaterstaat (the executive Directorate General for Public Works and Water Management of the Dutch Government) and the Dutch Water Boards for the purpose of creating a height model for the Netherlands (Van Der Zon, 2013).

The AHN2 dataset that was used in this research was collected between 1 February 2009 and 12 April 2009, a period that was characterised by low temperatures, low-hanging clouds and abundant precipitation until the second week of March (Leusink and Dijkman, 2010). The dataset, separated in different units each representing a part of the Netherlands, could be freely downloaded from www.nationaalgeoregister.nl. To cover the whole study area, only unit 06hz1 was needed. Two different AHN2 point cloud datasets of unit 06hz1 were available: an unclassified filtered point cloud dataset that contained all measured points at the ground level and an unclassified filtered out point cloud dataset that contained all measured points above the ground level. Both datasets were downloaded.

To process the LiDAR point cloud datasets, LAStools, a freely available software package developed by Martin Isenburg was used. The LAStools package was downloaded from http://rapidlasso.com/lastools/. Although LAStools is a free-standing software product that can be used without support of other software, it was used in combination with ArcGIS 10.2 in this research. The ArcGIS 10.2 software package was provided by Wageningen UR GeoDesk.

Aerial photographs were used to check the data and to create an NDVI map. Since high resolution aerial photographs made at the same time as the LiDAR point cloud collection are only available for Rijkswaterstaat and the Dutch Water Boards, the owners of the AHN2 dataset (Van Der Zon, 2013), photographs needed to be obtained in a different way. For the study area, a false colour aerial photograph with a resolution of 25 cm and aerial photographs with a resolution of 50 cm of the years 2008, 2009, 2010 and 2014 were provided by Wageningen UR GeoDesk.

2.3 Pre-processing the LiDAR point cloud data

To satisfy the starting point of the research objective, creating a data processing model from an **unclassified** LiDAR point cloud dataset, the filtered and filtered out datasets were merged to create an unclassified point cloud dataset containing all the collected LiDAR points. For this, the *lasmerge* tool was used. The resulting dataset was clipped to the boundary of the study area with the help of

the *lasclip* tool. A buffer of 100 m around the study area was created to prevent inaccuracies at the study area boundary. Then, duplicate points were removed with the help of the *lasduplicate* tool and noise points were removed with the help of the *lasnoise* tool. The resulting pre-processed dataset could be used for further modelling. Figure 7 shows the flow chart of the pre-processing phase.

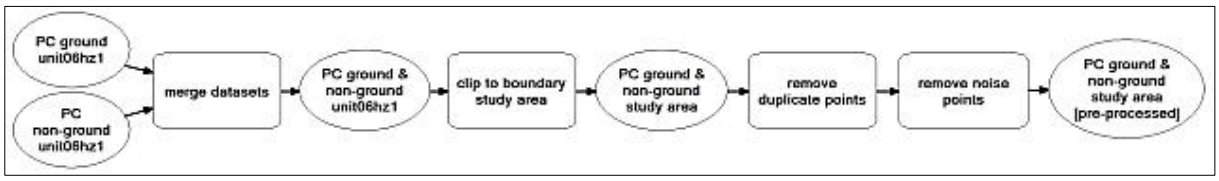

Figure 7: Flow chart of the pre-processing phase of the AHN2 LiDAR data

2.4 Visual analysis of the LiDAR point cloud dataset

Before continuing to the next modelling step, a visual analysis of the LiDAR point cloud dataset was carried out to see if it was possible to distinguish the different small green landscape elements from their surrounding environment and from each other by looking at the LiDAR point cloud data only. For this, profiles of the 26 small green landscape elements that were identified in the study area (see Chapter 3.1 for an overview of these elements) were analysed.

In the classification tree in Figure 4, it was shown that a small green landscape element belongs to a wooded bank when the vegetation grows on top of a wall of earth. It was hypothesized that a wall of earth should be visible in a cross section and therefore cross sections were made of all the identified small green landscape elements in the study area.

Shelterbelts, alder belts and rows of trees can be distinguished from each other through the presence or absence of a shrub layer. Whereas shelterbelts have a shrub layer, alder belts and rows of trees lack the presence of a shrub layer and exist only of trees. A shrub is defined as "*a low-growing woody plant with many stems rather than one trunk*", whereas a tree is defined as "*a woody plant, usually over 25 meters tall, with one to a few main stems and many branches*" (http://forestry.usu.edu/htm/treeid/tree-and-botanical-glossary/; Figure 8). It was hypothesized that the presence of stems or shrub layers should be visible in a side view and therefore side views were made of all the small green landscape elements that were identified in the study area.

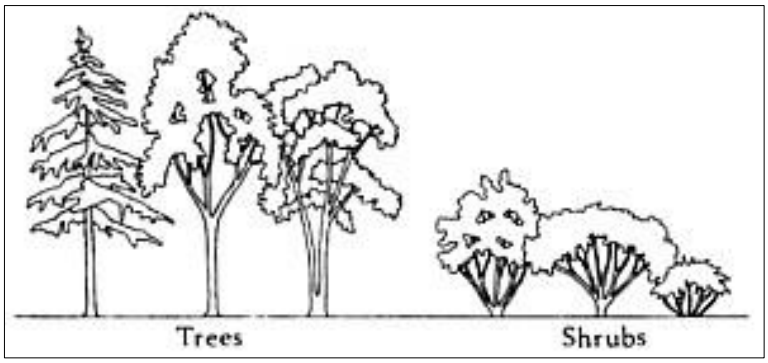

Figure 8: Tree versus shrub (source: http://eu.lib.kmutt.ac.th/elearning/Courseware/ARC261/chapter4_1.html)

The pre-processed LiDAR point cloud dataset was used to visualise the cross sections and the side views. First, the noise class was removed from the dataset with the help of the *las2las (filter)* tool, after which the dataset was clipped to the boundary of each small green landscape element with the help of the *lasclip* tool. The boundaries of the landscape elements were determined manually and are shown in Appendix 1. Each dataset was then converted from a LAZ file to a LAS file with the help of the *laszip* tool, after which a LAS dataset was created from each LAS file. In total, 26 LAS datasets were created. Finally, ArcGIS 10.2 was used to visualise each LAS dataset with the help of the *profile view* tool from the LAS Dataset toolbar. Figure 9 shows the flow chart for creating the LAS datasets.

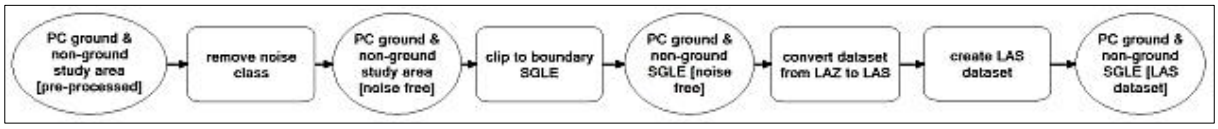

Figure 9: Flow chart for creating the LAS datasets that are used for visual analysis

2.5 Creating the data processing model

The general objective of this thesis research was to examine if unclassified point cloud LiDAR data could be used to create a data processing model that is able to detect small green landscape elements in the Netherlands. In this paragraph it is explained how the data processing model was created and validated.

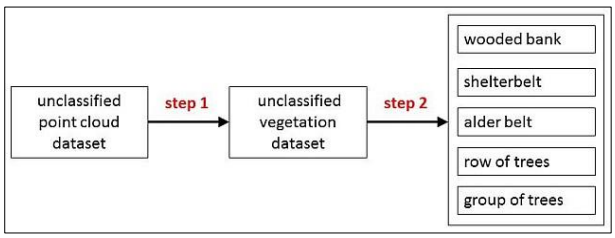

Figure 10: Steps that were taken to create the data processing model

As shown in Figure 10, the data processing model is built up in two steps. In the first step, an unclassified LiDAR point cloud dataset was created containing all the vegetation points that were filtered from the original unclassified LiDAR point cloud dataset. In the second step, the small green landscape elements were classified from the unclassified vegetation dataset that was created in the first step.

2.5.1 Creating the unclassified vegetation dataset (step 1)

To create the unclassified point cloud vegetation dataset, the pre-processed LiDAR point cloud dataset was used. Figure 11 shows the flow chart for creating the unclassified vegetation dataset. First, ground points were classified with the help of the *lasground* tool. To determine the parameters for terrain type and granularity, a trial-and-error method was used. Terrain type '*towns or flats'* with a default granularity was found to give the best results. After ground classification, height of the non-ground points relative to the ground points were calculated with the help of the *lasheight* tool and buildings and high vegetation were classified with the help of the *classify* tool. The resulting dataset

was then normalized with the help of the *lasheight* tool in which all ground points were assigned a height of zero meters and all values below zero meters were removed from the dataset.

To make sure that possible misclassified LiDAR points would not disturb the final vegetation dataset, Normalized Difference Vegetation Index (NDVI) was used to remove all non-vegetation points from the normalized dataset. NDVI is the most common used and preferred index for vegetation extraction. The index is based on the fact that green vegetation reflects more near-infrared light than visible light, whereas sparse or less green vegetation reflects more visible light than near-infrared light. NDVI calculation results in a ratio between -1 and +1 where positive values correspond to vegetation zones and negative values correspond to non-vegetation zones (Yengoh *et al*., 2014).

Using the raster calculator from ArcGIS 10.2, an NDVI map was created from a false colour aerial photograph of 2008 with the formula:

$$NDVI = (NIR - RED) / (NIR + RED)$$

where NIR represents the reflectance in the near-infrared band and RED represents the reflectance in the visible red band. The NDVI map was then reclassified in two classes with the help of the *reclassify* tool: a vegetation class (all values above zero) and a non-vegetation class (all values below zero). After that, the non-vegetation elements were selected from the reclassified file with the help of the *extract by attributes* tool and converted to polygons with the help of the *raster to polygon* tool. The polygons were used to remove the non-vegetation points from the normalized LiDAR dataset with the help of the *lasclip* tool.

After removing the non-vegetation points from the normalized dataset with the help of NDVI, the *las2las (filter)* tool was used to remove all the earlier created non-vegetation classes (unclassified, ground, buildings and noise) from the normalized dataset. Finally, a point shapefile containing the unclassified vegetation points was created with the help of the *las2shp* tool and a polygon shapefile containing the vegetation boundaries was created with the help of the *lasboundary* tool. For the best fitting of the vegetation boundaries, the concavity was set to 4,0.

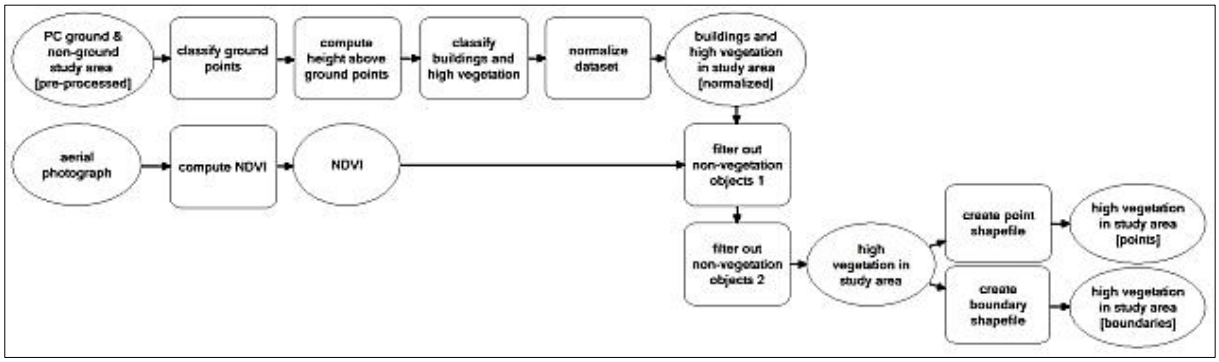

Figure 11: Flow chart for creating the unclassified vegetation dataset

2.5.2 Statistical analysis of the LiDAR point cloud dataset

The next step was to identify and classify the different small green landscape elements from the unclassified vegetation dataset. Characteristic parameters of each small green landscape element needed to be determined that could be used for classification. For this, statistical analyses were performed on the LiDAR point cloud datasets of 13 randomly selected small green landscape elements in the study area (training data). All uneven numbered small green landscape elements were used for training, except for row of trees 3 and group of trees 3. During the visual analysis, the point clouds of these two small green landscape elements were found to be too unreliable and it was therefore decided to remove them from the training dataset.

All LiDAR points below a height of 0,25 m were removed from the unclassified LiDAR point cloud vegetation dataset, with the help of the *lasheight* tool, to prevent possible misclassified ground points to pollute the dataset. The point cloud dataset was then clipped to the boundaries of each small green landscape element with the help of the *lasclip* tool. The boundaries of these elements were determined manually and were the same boundaries as used during the visual analysis. Finally, the 13 resulting datasets were each converted to ASCII text files, containing all the height points (*z*-values) of each small green landscape element, with the help of the *las2txt* tool.

From the ASCII text files, maximum height, mean height, median height, variance, standard deviation, standard error, skewness and kurtosis were calculated in Microsoft Excel and compared between the different small green landscape elements to see if there were significant differences that could be used for classification. For shelterbelts and alder belts, average values from all the elements of each landscape element type (five shelterbelts and five alder belts) were used.

However, caution was needed in relation to the use of formulas to calculate skewness and kurtosis. Whereas LAStools uses the same formulas as FUSION, a LiDAR data analysis software package developed by the Forest Service of the US Department of Agriculture (source: Martin Isenburg, https://groups.google.com/d/msg/lastools/lfHz561d2Zw/mHma_0bheRsJ), Microsoft Excel uses slightly different formulas, leading to different calculation results. The difference lies in the fact that the kurtosis values calculated by LAStools are reduced by three when the Microsoft Excel formula is used so that the kurtosis value for a standard normal distribution becomes zero instead of three (NIST/SEMATECH, 2012). Moreover, the formulas used by Microsoft Excel include an adjustment for sample size (Doane and Seward, 2011), whereas the formulas used by LAStools do not. For uniformity it was decided not to use the standard formulas from Microsoft Excel but the formulas from LAStools instead. Since the results of the formulas used in LAStools and the adjusted formulas

used in Microsoft Excel are similar when sample sizes are large (Doane and Seward, 2011), the LAStool formulas could be used without problems in this research.

For skewness the following formula was used: $\frac{\sum_{i=1}^{n}(y_i - y_{mean})^3}{(n-1)s^3}$ (McGaughey, 2014)

For kurtosis the following formula was used: $\frac{\sum_{i=1}^{n}(y_i - y_{mean})^4}{(n-1)s^4}$ (McGaughey, 2014)

where n = number of LiDAR data points
y_i = LiDAR data point
y_{mean} = mean value of all LiDAR data points
s = standard deviation

2.5.3 Classifying the small green landscape elements (step 2)

To classify the small green landscape elements, the unclassified LiDAR point cloud vegetation dataset that was created in the first step was used. The flow chart for classifying the small green landscape elements is shown in Figure 12.

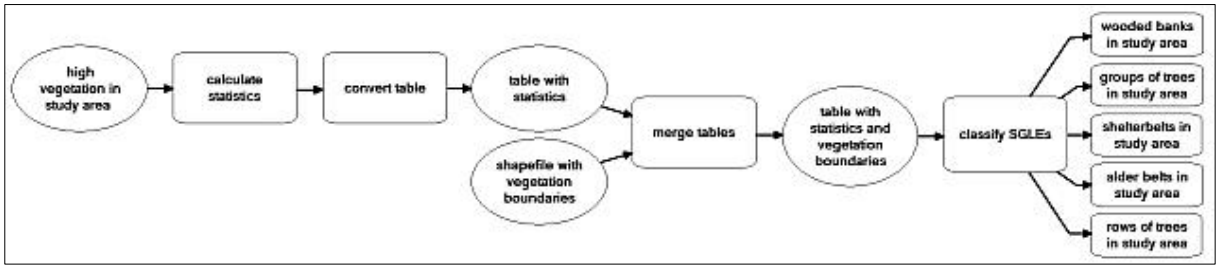

Figure 12: Flow chart for classifying the small green landscape elements

First, maximum height, mean height, standard deviation, skewness and kurtosis of each small green landscape element in the training dataset were calculated and stored in a table with the help of the *lascanopy* tool. The polygon shapefile with the boundaries of the small green landscape elements, which was created in the first step, was used to determine the boundaries of the small green landscape elements within which the statistics needed to be calculated. Then, the table containing the statistical results was merged with the table of the polygon shapefile containing the vegetation boundaries with the help of the *join field* tool. Since the statistics table did not have ObjectIDs assigned, it had to be converted to a dBase table first with the help of the *table to table* tool. After merging the tables, the small green landscape elements were classified with the help of the *select* tool. The selection criteria for the classification based on the results of the statistical analysis (see Chapter 3.3.2 for the results) are shown in Table 1.

Table 1: Selection criteria for the classification of small green landscape elements in the study area

statistic type	wooded bank	group of trees	shelterbelt	alder belt	row of trees
maximum height	≥ 15	≥ 15	< 15	< 15	≥ 15
mean height	< 7	≥ 7	< 7	≥ 7	≥ 7
standard deviation	≥ 4	< 4	< 4	< 4	≥ 4
skewness	≥ 0	< 0	≥ 0	< 0	< 0
kurtosis	< 3	< 3	≥ 3	< 3	< 3

2.6 Validating the data processing model

To validate the data processing model, the complete model (see Appendix 2 for an overview of the model) was run on the unclassified LiDAR point cloud dataset of the whole study area, after which an accuracy assessment could be carried out on the small green landscape elements that were identified during the field inventory. Since data that is used for an accuracy assessment needs to be independent from training data (Congalton, 2001), it was important to use only the even numbered small green landscape elements for the accuracy assessment since uneven numbered small green landscape elements were already used for training. It was decided, however, to remove row of trees 2 and group of trees 2 from the accuracy assessment dataset because the visual analysis had shown that the point clouds of these two small green landscape elements were too unreliable.

For the accuracy assessment, an error matrix had to be created. From the error matrix, overall accuracy, user's accuracy and producer's accuracy could be calculated. An example of an error matrix with the calculation of the overall accuracy, user's accuracy and producer's accuracy is shown in Figure 13. Whereas user's accuracy indicates the probability that a polygon classified on the map actually represents that category in the field, producer's accuracy indicates the probability that a reference polygon is being correctly classified (Congalton, 2001).

Overall accuracy is calculated by dividing the total number of correct classified polygons (the sum of the major diagonal) by the total number of polygons in the error matrix. User's accuracy is calculated by dividing the total number of correct classified polygons in a category by the total number of polygons that are classified in that category (the row total). Producer's accuracy is calculated by dividing the total number of correct classified polygons in a category by the total number of polygons of that category as derived from the reference data (the column total).

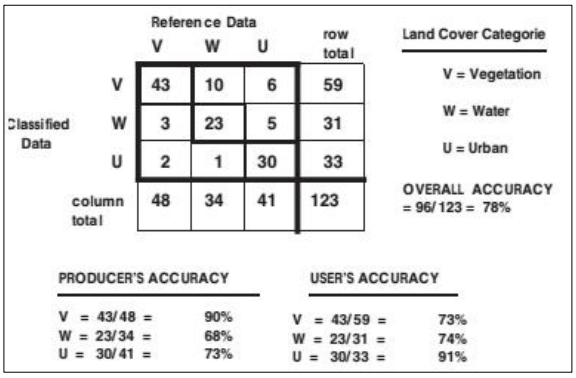

Figure 13: Example of an error matrix with the calculation of overall accuracy, user's accuracy and producer's accuracy (source: Congalton, 2001)

3 Results and discussion

In Chapter 3 the results of this thesis research are shown and discussed. First, the results of the study area inventory are discussed, followed by a discussion of the results of the visual analysis of the LiDAR point cloud dataset. Finally, the results of the creation and validation of the data processing model are discussed. A discussion about the results of the statistical analysis of the LiDAR point cloud dataset is included in the discussion of the creation and validation of the data processing model.

3.1 Inventory of the study area

3.1.1 Inventory of small green landscape elements

The vegetation in the study area mainly consists of native species with black alder (*Alnus glutinosa*) being the dominating tree type. Shrub types were difficult to determine due to the absence of leaves but most likely consist of blackthorn (*Prunus spinosa*) or common hawthorn (*Crataegus monogyna*). Five different small green landscape element types were identified during the field inventory: wooded bank (2x), shelterbelt (9x), alder belt (9x), row of trees (3x) and group of trees (3x). Based on the Index Nature and Landscape (Index Natuur en Landschap, onderdeel Landschapsbeheertypen, version 2015) and field observations, the small green landscape elements can be described as follow:

Wooded bank

A wooded bank is a detached linear shaped and continuous landscape element with an ascending vegetation of native trees and/or shrubs that are situated on a wall of earth. The maximum width of a wooded bank is 20 m. The vegetation is managed as coppice wood.

Group of trees

A group of trees is a detached polygonal shaped and continuous landscape element with an ascending vegetation of native trees and/or shrubs. The surface of a group of trees ranges between two are and one hectare.

Shelterbelt

A shelterbelt is a detached linear shaped and continuous landscape element with an ascending vegetation of native trees and/or shrubs that are not situated on a wall of earth. The maximum width of a shelterbelt is 20 m. The vegetation is managed as coppice wood.

Alder belt

An alder belt is a detached linear shaped and continuous single rowed landscape element that mainly exists of black alder (> 50 per cent occurrence). Shrubs do not occur. Alder belts are often situated next to ditches. The vegetation is managed as coppice wood.

Row of trees

A row of trees is a detached linear shaped landscape element existing of native deciduous trees, situated next to or on agricultural land. Black alder does not dominate the element (< 50 per cent occurrence). The minimum amount of trees is eight trees per 100 m. Shrubs do not occur.

An overview of the locations of the small green landscape elements that were found in the study area is shown in Figure 14. In Appendix 1, top views of these landscape elements are shown. Shelterbelts and alder belts are the dominating small green landscape elements. Wind belts and pollard willow (*Salix alba*) rows, classified as separate small green landscape elements in the Index Nature and Landscape (Index Natuur en Landschap, onderdeel Landschapsbeheertypen, version 2015), were also found in the study area but since only one wind belt and only two pollard willow rows were found, it was decided to assign them to respectively group of trees and row of trees.

Figure 14: Overview of small green landscape elements in the study area (orange = wooded bank, green = group of trees, purple = shelterbelt, blue = alder belt, yellow = row of trees)

Figure 15: Overview of tree height measurement locations in the study area (blue = black alder, yellow = sessile oak, purple = pollard willow)

3.1.2 Measuring tree heights

Tree heights from three different tree types were determined at 23 randomly chosen locations in the study area (Figure 15). Moreover, shrub heights were determined at five randomly chosen locations (indicated with a white asterisk [*] in Figure 15). While the heights of black alder and sessile oak (*Quercus petraea)* had to be estimated using an inclinometer, the heights of the pollard willows and shrubs could be measured using a measuring tape.

Heights of black alder (17 examined trees) range between 6,2 m and 17,4 m with a mean height of 11,3 m, while heights of sessile oak (three examined trees) range between 8,2 m and 31,2 m with a mean height of 19,4 m. Heights of pollard willows, which could be measured because they were clipped, are 1,8 m. Shrub heights range between 1,5 m and 2,5 m with a mean height of 2,1 m.

3.1.3 Discussion

A large part of the study area was inaccessible due to the absence of public roads and paths and the presence of ditches, electric barbed wires, and private properties, roads and paths. The inventory was therefore mainly carried out in the central part of the study area, also known as 'Het Curringherveld'. A decrease in the total area that can be used for the inventory limits the total amount of small green landscape elements that can be identified and used for validation. For validation with the help of an error matrix it is advised to use at least 30 samples per map class to adequately populate an error matrix (Congalton, 2001). In this research, 26 small green landscape elements were identified in the study area, which is far below the minimum sample size as advised by Congalton (2001). The results from the error matrix might therefore not be reliable.

Tree heights were estimated to see if LiDAR point cloud heights did not deviate too much from field heights. Since a time gap of six years exists between LiDAR point cloud collection (2009) and field inventory (2015) it is likely that LiDAR point cloud heights are lower than field heights because of natural growth of the trees. However, estimated heights of black alder could still be used for comparison because most trees in the study area exist of mature trees. Whereas highest annual growth of black alder occurs between the age of four and ten with an annual growth rate of 1,5 m, growth rates slow down rapidly once black alder matures (Claessens *et al.*, 2010). It was therefore assumed that as long field heights did not deviate more than nine meters from LiDAR point cloud heights, differences in height were not significant.

3.2 Visual analysis of the LiDAR point cloud dataset

3.2.1 Visual analysis of wooded banks

Two wooded banks were identified in the study area. Their locations are shown in Figure 16.

Figure 16: Wooded bank locations in the study area

Wooded bank 1 (WB1) has a wall of earth with a height of 1,2 m and a width of 3,0 m. Trees on top of the wall exist of sessile oak, black alder and some unidentified species. Maximum height of the wooded bank in the normalized vegetation dataset is 15,74 m. One of the sessile oaks that were measured during the field visit had an estimated height of 8,2 m. Since the difference is less than nine meters, it is not significant and the height of the wooded bank in the vegetation dataset is considered reliable.

Wooded bank 2 (WB2) has a grass covered wall with a height of 0,7 m and a width of 2,0 m. Trees on top of the wall mainly exist of sessile oak. Maximum height of the wooded bank in the normalized vegetation dataset is 19,52 m. One of the sessile oaks that were measured during the field visit had an estimated height of 18,8 m. Since the difference is less than nine meters, it is not significant and the height of the wooded bank in the vegetation dataset is considered reliable.

The main characteristic of a wooded bank is a wall of earth, a local elevation of the ground level in the landscape. In a profile of the LiDAR point cloud data this elevation should be visible. The cross sections of both wooded bank 1 and wooded bank 2 indeed show an elevation in the landscape, indicating the presence of a wall of earth (Figure 17).

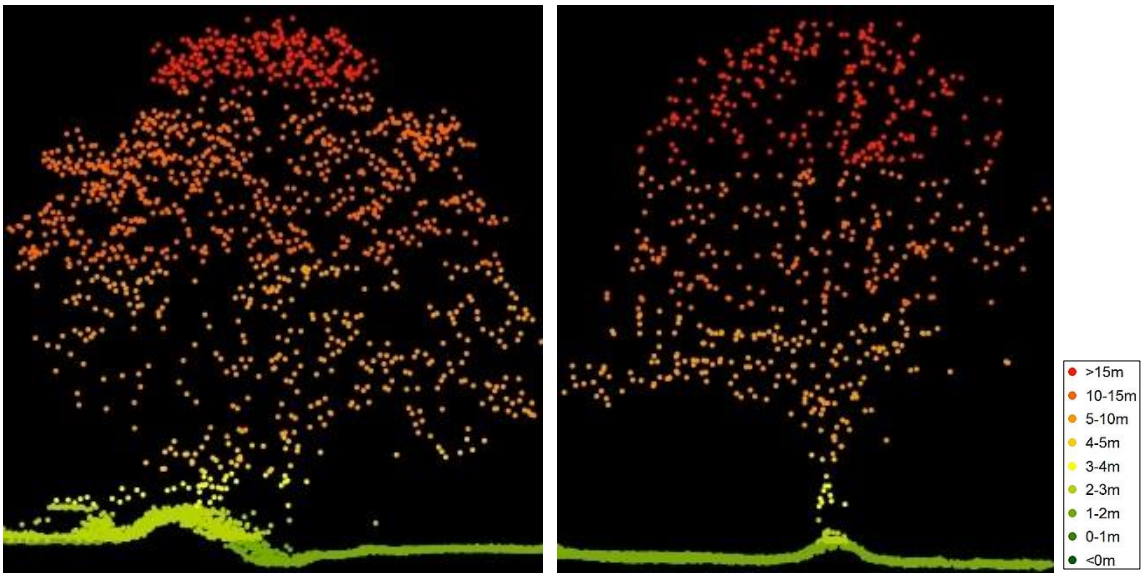

Figure 17: Cross sections of wooded bank 1 (left) and wooded bank 2 (right) with the presence of a wall of earth

The visible absence of stems and the higher point density at stem level in the side view of wooded bank 1 (Figure 18) indicates that this wooded bank exists of trees and shrubs. In the side view of wooded bank 2 (Figure 19) stems are clearly visible. Moreover, point density under the tree crowns is low, indicating that this wooded bank mainly exists of trees.

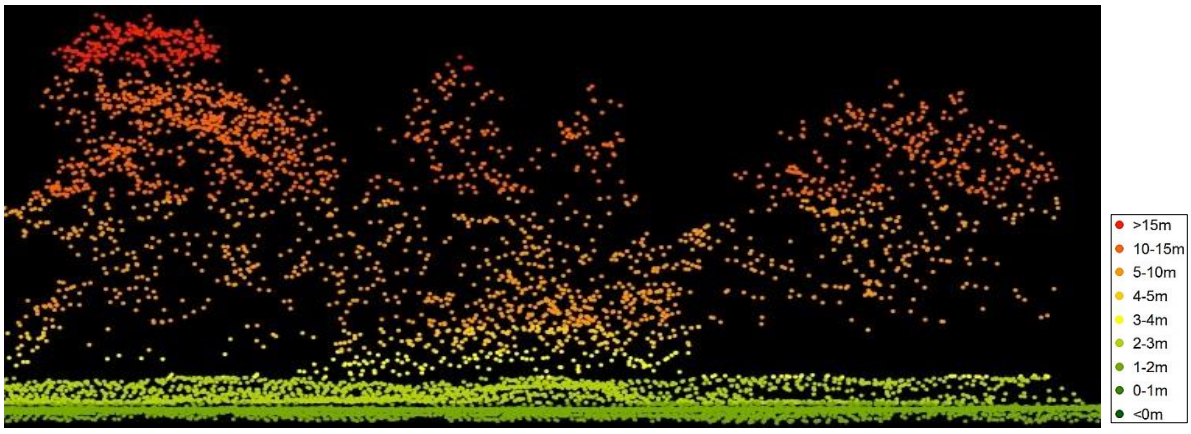

Figure 18: Side view of wooded bank 1 (WB1)

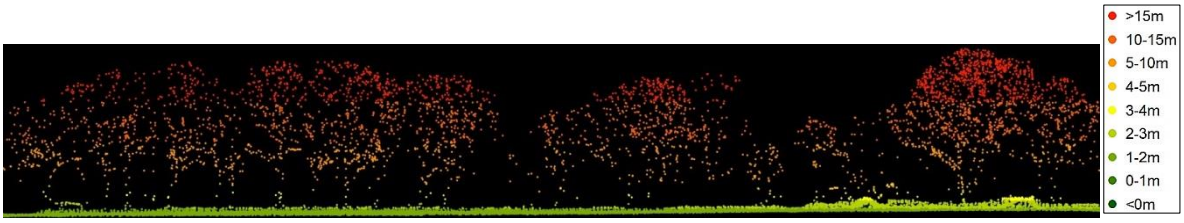

Figure 19: Side view of wooded bank 2 (WB2)

3.2.2 Visual analysis of groups of trees

Three groups of trees were identified in the study area. Their locations are shown in Figure 20.

Figure 20: Group of trees locations in the study area

Group of trees 1 (GoT1) concerns a wind belt around a house, existing of different tree and shrub species. The group of trees is surrounded by a fence that is partly covered with ivy (*Hedera helix*). Maximum height of the group of trees in the normalized vegetation dataset is 20,21 m.

Group of trees 2 (GoT2) exists of black alder, at two sides surrounded by a plaited mat of willow-wood with a height of 1,0 m. Shrubs do not occur. Maximum height of the group of trees in the normalized vegetation dataset is 5,40 m. One of the black alders that were measured during the field visit had an estimated height of 10,7 m. Since the difference is less than nine meters, it is not significant and the height of the group of trees in the vegetation dataset is considered reliable.

Group of trees 3 (GoT3) exists of black alder and other unidentified tree types situated in and around a little pond in between two shelterbelts. Tree stems are thin. Maximum height of the group of trees in the normalized vegetation dataset is 3,76 m.

The main characteristic of a group of trees is the polygonal shape of the group. The boundaries of the vegetation elements in Figure 20 are indeed polygonal shaped, indicating that the vegetation elements are groups of trees. The absence of a wall of earth in the cross sections of Figure 21 indicates that the vegetation elements are not wooded banks, but could be groups of trees.

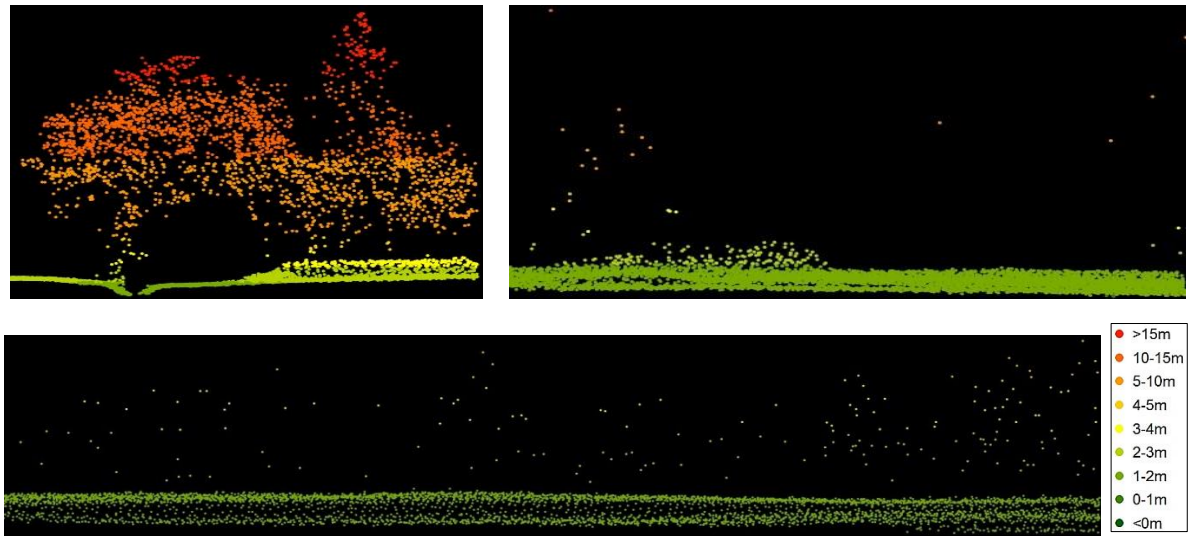

Figure 21: Cross sections of group of trees 1 (top left), group of trees 2 (top right) and group of trees 3 (bottom)

However, although the polygonal boundary shapes and absence of a wall of earth indicate that the vegetation exists of groups of trees, for the side views this is not so obvious. Whereas the side view of group of trees 1 in Figure 22 clearly shows a group of trees, in particular at the right side of the house, for the side views of group of trees 2 (Figure 23) and group of trees 3 (Figure 24) this is not clear. In these side views, the few points that are visible above the ground do not indicate the presence of tree groups.

Figure 22: Side view of group of trees 1 (GoT1)

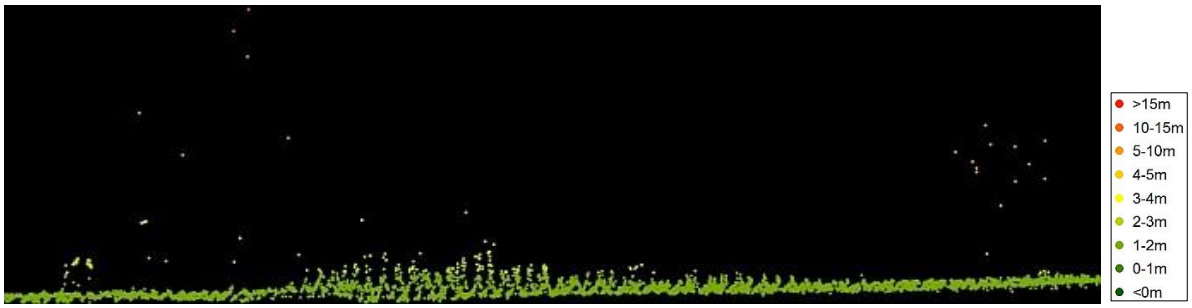

Figure 23: Side view of group of trees 2 (GoT2)

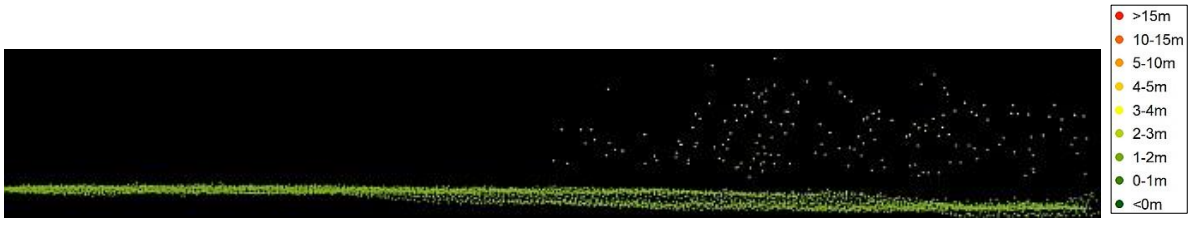

Figure 24: Side view of group of trees 3 (GoT3)

The absence of trees in group of trees 2 and group of trees 3 is strengthened by the shape of the histograms shown in Figure 25. Most LiDAR points are found between a height of 1,0 to 2,0 m and just a few LiDAR points are found higher. Since height class distribution in the histograms starts at 1,0 m, these LiDAR points most likely belong to the ground and not to trees.

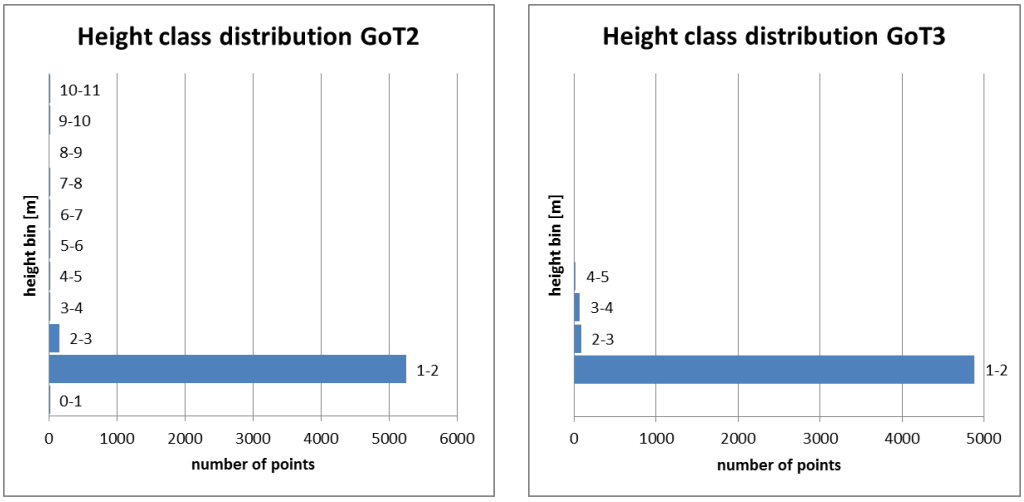

Figure 25: Histograms of the height class distribution of group of trees 2 (left) and group of trees 3 (right)

3.2.3 Visual analysis of shelterbelts

Nine shelterbelts were identified in the study area. Their locations are shown in Figure 26.

Figure 26: Shelterbelt locations in the study area

The shelterbelts mainly exist of black alder, sometimes in combination with sessile oak or unidentified species, with a layer of shrubs. Maximum shelterbelt heights in the normalized vegetation dataset range from 11,17 m to 20,48 m. None of the estimated tree heights, measured during the field visit, differ more than nine meters from the heights in the vegetation dataset and the heights of the shelterbelts in the vegetation dataset are therefore considered reliable. An overview of the shelterbelt heights in the vegetation dataset and the estimated tree heights is shown in Table 2.

Table 2: Overview of shelterbelt heights [m NAP] according to the LAS datasets and estimated tree heights [m] as measured during the field visit

shelterbelt number	shelterbelt height [m NAP]	estimated tree height [m]
1	11,58	10,5 (black alder) 13,3 (black alder)
2	14,22	10,3 (black alder) 6,2 (black alder) 7,0 (black alder)
3	18,47	9,6 (black alder)
4	20,48	--
5	13,13	9,7 (black alder) 10,2 (black alder)
6	14,00	--
7	11,17	--
8	13,81	6,4 (black alder) 11,5 (black alder) 12,0 (black alder)
9	15,20	--

The main characteristic of a shelterbelt is the presence of a shrub layer. Although a wooded bank and a group of trees can also have a shrub layer, a shelterbelt can be distinguished from these two landscape elements by the absence of a wall of earth and the linear instead of polygonal shape of the belts. In Figure 26, the linear shapes of the shelterbelts are clearly visible. The cross sections in Figure 27 show that, except for the cross sections of shelterbelt 1 (SB1) and shelterbelt 8 (SB8), the shelterbelts are not situated on a wall of earth. The cross sections of shelterbelt 4 (SB4) and shelterbelt 6 (SB6) even show a local lowering of the ground level, indicating the presence of a ditch.

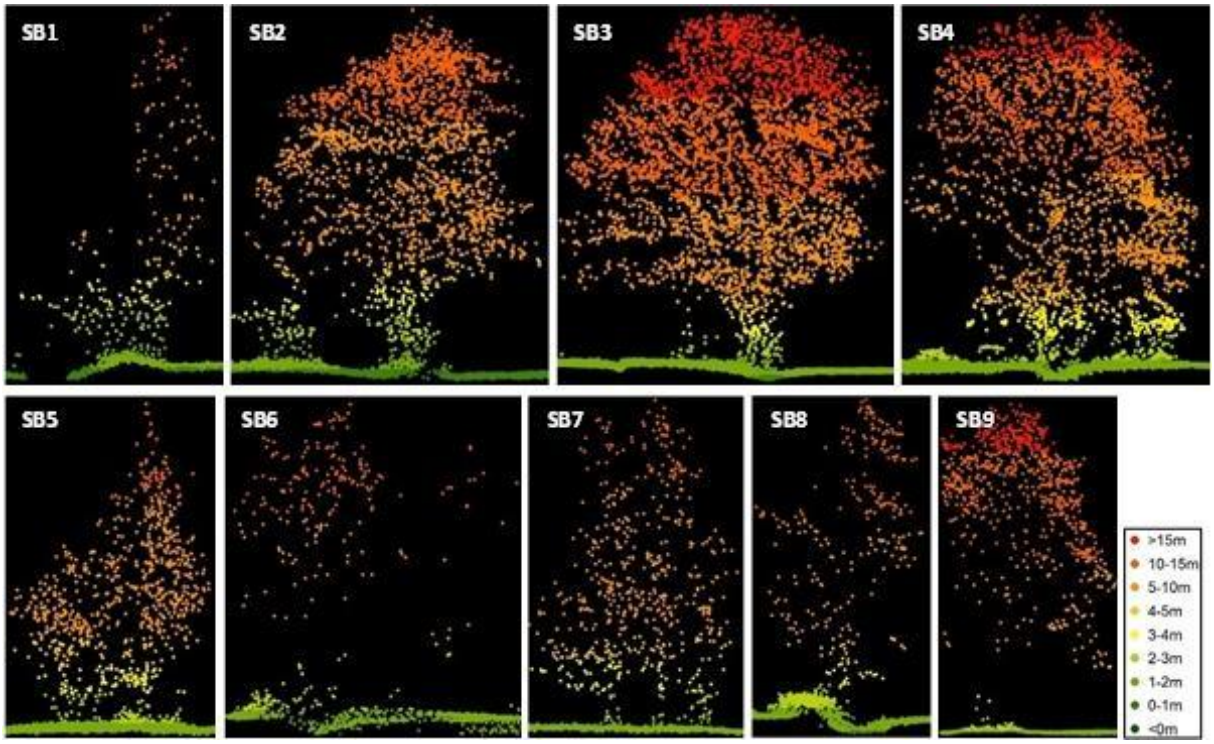

Figure 27: Cross sections of the shelterbelts in the study area

Figure 28 to Figure 36 show the side views of the shelterbelts. In all Figures, trees can be distinguished from the LiDAR point clouds. Shrub layers should be visible in a side view as a high point density at tree stem level. Point density at stem level in all Figures, except for Figure 35 and Figure 36, is high, indicating the presence of a shrub layer. Point density at stem level in Figure 35 and Figure 36 is low and it is therefore not possible to state with certainty that shrub layers occur in these belts and that the LiDAR point clouds indeed represent shelterbelts.

Figure 28: Side view of shelterbelt 1 (SB1)

Figure 29: Side view of shelterbelt 2 (SB2)

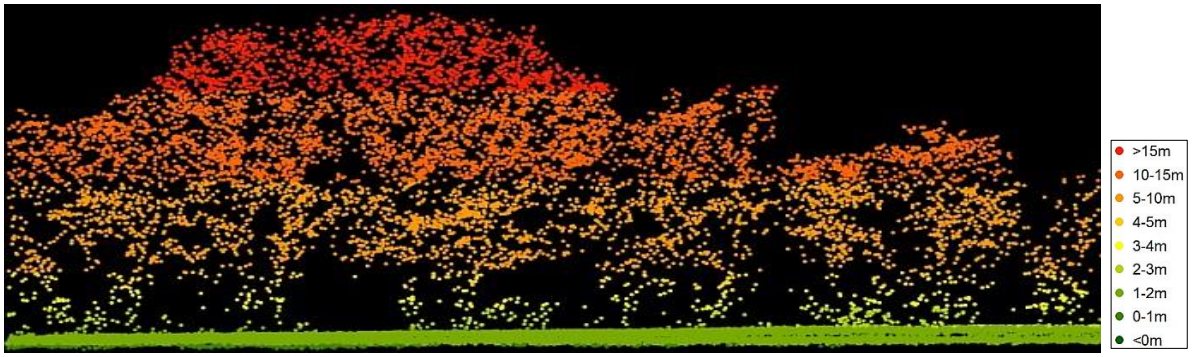

Figure 30: Side view of shelterbelt 3 (SB3)

Figure 31: Side view of shelterbelt 4 (SB4)

Figure 32: Side view of shelterbelt 5 (SB5)

Figure 33: Side view of shelterbelt 6 (SB6)

Figure 34: Side view of shelterbelt 7 (SB7)

Figure 35: Side view of shelterbelt 8 (SB8)

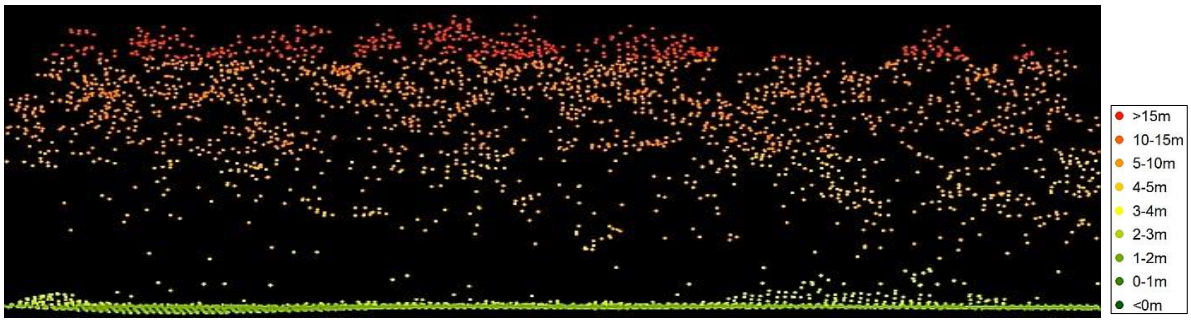

Figure 36: Side view of shelterbelt 9 (SB9)

The photographs in Figure 37, taken at 24 March 2015, show the current appearance of shelterbelt 8 and shelterbelt 9. The photographs show a uniform distribution of trees and underlying shrub layers for both shelterbelts. This distribution is not visible in Figure 35 where only a few trees (with shrub layers) are present and in Figure 36 where point density is highest in the upper layers and tree crowns sometimes seem to "float" due to the lack of LiDAR points underneath the crowns.

Figure 37: Current appearance of shelterbelt 8 (left) and shelterbelt 9 (right) (photographs taken at 24.03.2015)

3.2.4 Visual analysis of alder belts

Nine alder belts were identified in the study area. Their locations are shown in Figure 38.

Figure 38: Alder belt locations in the study area

The alder belts mainly exist of black alder, sometimes in combination with sessile oak or unidentified species. A shrub layer is absent. Maximum alder belt heights in the normalized vegetation dataset range from 11,49 m to 17,37 m. None of the estimated tree heights, measured during the field visit, differ more than nine meters from the heights in the vegetation dataset and the heights of the alder belts in the vegetation dataset are therefore considered reliable. An overview of the alder belt heights and the estimated tree heights is shown in Table 3.

Table 3: Overview of alder belt heights [m NAP] according to the LAS dataset and estimated tree heights [m] as measured during the field visit

alder belt number	alder belt height [m NAP]	estimated tree height [m]
1	13,84	13,3 (black alder)
2	17,37	17,4 (black alder)
3	14,01	16,6 (black alder)
4	11,49	9,8 (black alder) 16,3 (black alder)
5	13,77	--
6	13,52	--
7	15,51	--
8	15,31	--
9	13,52	--

The main characteristics of an alder belt are the dominant presence of black alder and the absence of shrub layers. Although shrub layers can also be absent in a wooded bank or a group of trees, these landscape elements can be distinguished from an alder belt by the presence of a wall of earth (wooded bank) or by a polygonal instead of a linear shaped vegetation boundary (group of trees). The linear boundary shapes of the alder belts are clearly visible in Figure 38. The cross sections of the alder belts in Figure 39 do not show local elevations of the ground level, which indicates that a wall of earth is not present. In some of the cross sections, a local lowering of the ground level is visible, which indicates the presence of a ditch.

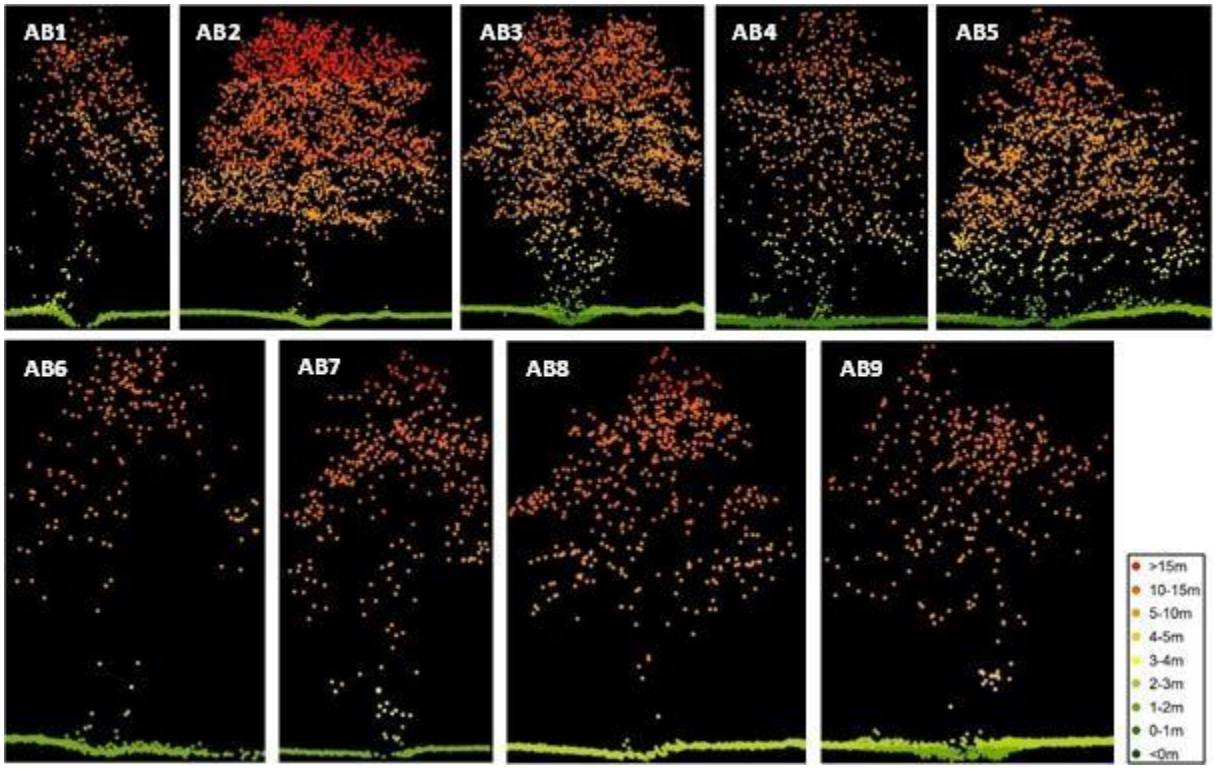

Figure 39: Cross sections of the alder belts in the study area

In Figure 40 to Figure 48, side views of the alder belts are shown. In most Figures, point density at stem level is low, indicating the absence of shrub layers. In these Figures, tree crowns and stems are clearly visible. In Figure 42, Figure 43 and Figure 44, however, a higher point density at stem level is visible, which might indicate the presence of a shrub layer. During the field inventory in the study area, some blackberry shrubs (*Rubus sp*.) were indeed detected underneath the trees from alder belt 3 (Figure 49, left photograph). However, since the density of these shrubs was minimal and the trees were clearly lined up in a single row, the vegetation element was classified as alder belt anyway. The higher point density at stem level for alder belt 4 (Figure 49, right photograph) and alder belt 5 (no photograph available) is not caused by the presence of a shrub layer, but by the presence of multi stems of the trees themselves.

Figure 40: Side view of alder belt 1 (AB1)

Figure 41: Side view of alder belt 2 (AB2)

Figure 42: Side view of alder belt 3 (AB3)

Figure 43: Side view of alder belt 4 (AB4)

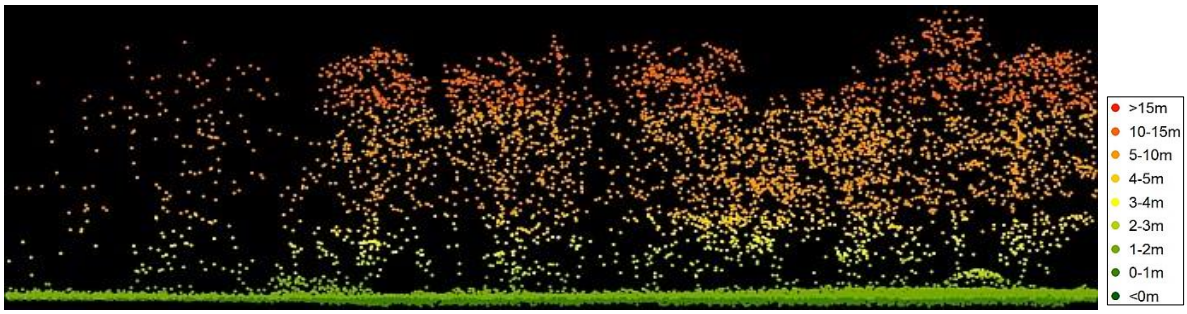

Figure 44: Side view of alder belt 5 (AB5)

Figure 45: Side view of alder belt 6 (AB6)

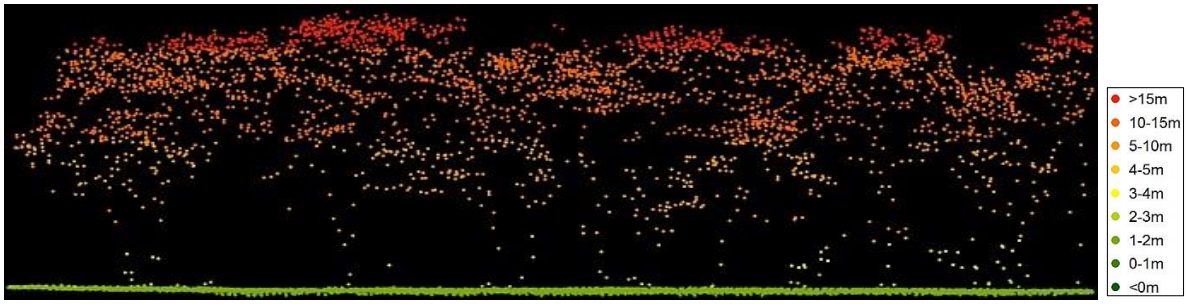

Figure 46: Side view of alder belt 7 (AB7)

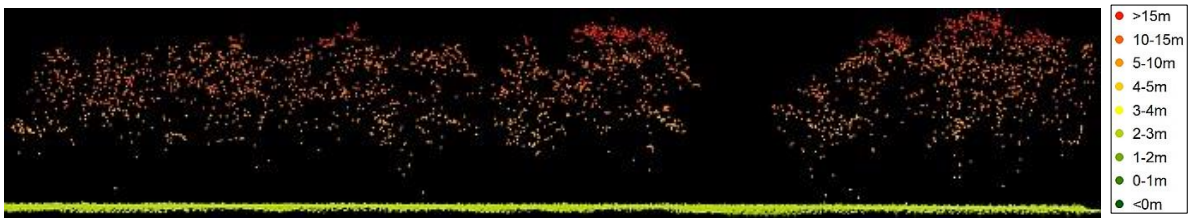

Figure 47: Side view of alder belt 8 (AB8)

Figure 48: Side view of alder belt 9 (AB9)

Figure 49: Current appearance of alder belt 3 (left) and alder belt 4 (right) (photographs taken at 08.03.2015)

3.2.5 Visual analysis of rows of trees

Three rows of trees were identified in the study area. Their locations are shown in Figure 50.

Figure 50: Row of trees locations in the study area

Row of trees 1 (RoT1) exists of a single row of sessile oaks, situated between a shed and a grassland. A shrub layer is absent. Maximum height of the row of trees in the normalized vegetation dataset is 17,58 m. One of the oaks that were measured during the field visit had an estimated height of 31,2 m, which is much higher than the maximum height of the row of trees in the normalized dataset. However, since it was not possible to measure the distance from the eye level to the sessile oak during the field visit, this distance was estimated later from Google Earth, and measuring errors might therefore have occurred when estimating the tree height.

Row of trees 2 (RoT2) and row of trees 3 (RoT3) both exist of a single row of pollard willows. Shrub layers are absent. At the time of the field visit, the pollard willows were clipped and only stems were visible. Row of trees 2 is situated next to a walking path, whereas row of trees 3 is situated next to a pond. All trees could be measured using a measuring tape. Heights of all trees as measured in the field are 1,8 m. According to the normalized vegetation dataset, however, maximum height of row of trees 2 is 11,11 m whereas maximum height of row of trees 3 is 4,09 m.

The main characteristic of a row of trees is the absence of a shrub layer. Moreover, a row of trees has a linear shape and the trees are not situated on a wall of earth. The absence of a wall of earth is clearly visible in the cross sections of the rows of trees in Figure 51.

Figure 51: Cross sections of row of trees 1 (upper left), row of trees 2 (bottom) and row trees 3 (upper right)

Side views of the rows of trees are shown in Figure 52, Figure 53 and Figure 54. In Figure 52, trees are clearly visible. In Figure 53 and Figure 54, however, the few LiDAR points that are visible in the point cloud do not indicate the presence of trees.

Figure 52: Side view of row of trees 1 (RoT1)

Figure 53: Side view of row of trees 2 (RoT2)

Figure 54: Side view of row of trees 3 (RoT3)

A row of trees can only be distinguished from an alder belt because the dominant vegetation type does not exist of black alder. Although this distinction is easy to make in the field, it is difficult to make this distinction in a LiDAR point cloud dataset. One option to distinguish the different small green landscape elements from each other is by looking at the shape of the individual trees. The silhouettes of the sessile oak and the black alder in Figure 55 show that the tree crown of a sessile oak is more or less circular shaped, whereas the tree crown of a black alder is more or less pyramid

shaped. In this research, however, distinguishing rows of trees based on individual tree shape is difficult because the trees in a row are often situated close to each other and tree crowns fuse.

Figure 55: Silhouette of a sessile oak (left) and a black alder (right) (source: www.floralimages.co.uk)

3.2.6 Discussion

In the visual analysis, it was shown that the LiDAR point clouds for some groups of trees, shelterbelts and rows of trees did not always show the presence of trees, even though these trees were identified during the field inventory. A reason for the absence of trees in the LiDAR point cloud datasets could be the large time gap between LiDAR point cloud collection (2009) and field inventory (2015). Vegetation is dynamic and changes from year to year due to natural processes as growth and death and human processes as planting, removing and cutting. It is therefore possible that trees were not present at the time of LiDAR point cloud collection but were planted later. Taking into consideration the low vegetation height and thin tree stems of group of trees 3, it looks indeed as if these trees were planted more recently.

To check if trees that were identified during the field inventory were indeed absent during LiDAR point cloud collection, high resolution aerial photographs from 2008, 2009, 2010 and 2014 were compared with each other. Although the quality of the photographs is sometimes low, they could still be used for comparison.

For group of trees 2 (Figure 57) and group of trees 3 (Figure 56), no significant differences occur between the different years, neither for group of trees 2 nor for group of trees 3. It can therefore be concluded that the large time gap between data collection and field inventory is not the reason for the absence of trees in the LiDAR point cloud datasets of these groups of trees. Obviously, there must be another reason. However, for now it is not clear what that reason might be.

Figure 57: Comparison of aerial photographs of 2008, 2009, 2010 and 2014 for group of trees 2

Figure 56: Comparison of aerial photographs of 2008, 2009, 2010 and 2014 for group of trees 3

When comparing the aerial photographs for the shelterbelts, no differences were found for shelterbelt 9 (Figure 58). For shelterbelt 8, however, a significant difference was found between the photographs of 2009 and 2014 (Figure 59). Whereas in the photograph of 2009 only a few individual tree crowns are visible in the upper part of the shelterbelt, the photograph of 2014 shows a continuous line of tree crowns in this part of the belt, indicating that extra trees were planted between LiDAR point cloud collection and field inventory.

Figure 58: Comparison of aerial photographs of 2008, 2009, 2010 and 2014 for shelterbelt 9

Figure 59: Comparison of aerial photographs of 2009 (left) and 2010 (right) for shelterbelt 8

Although sessile oaks were clearly visible in the side view of row of trees 1, pollard willows were not visible in the side views of row of trees 2 and row of trees 3. The aerial photographs of 2008 that are shown in Figure 60, however, show the presence of pollard willows at the locations of both rows of

trees, so the large time gap between LiDAR point cloud collection and field inventory is not the reason for the absence of the trees in the LiDAR point cloud dataset. Another reason for their absence could be that the pollard willows were clipped at the time of LiDAR point cloud collection and that the stems were too thin to be captured by the laser beam, but more research is needed to validate this reason.

Figure 60: Aerial photographs of 2008 with the presence of pollard willows in row of trees 2 (left) and row of trees 3 (right)

3.3 Creating the data processing model

3.3.1 Creating the unclassified vegetation dataset (step 1)

In the first step of modelling, a vegetation dataset was created from the unclassified LiDAR point cloud dataset. Initially, the vegetation dataset was created without the use of an NDVI filter, and although modelling results looked promising, some non-vegetation points turned out to be misclassified as vegetation points. These misclassified points are visible as red dots in Figure 61.

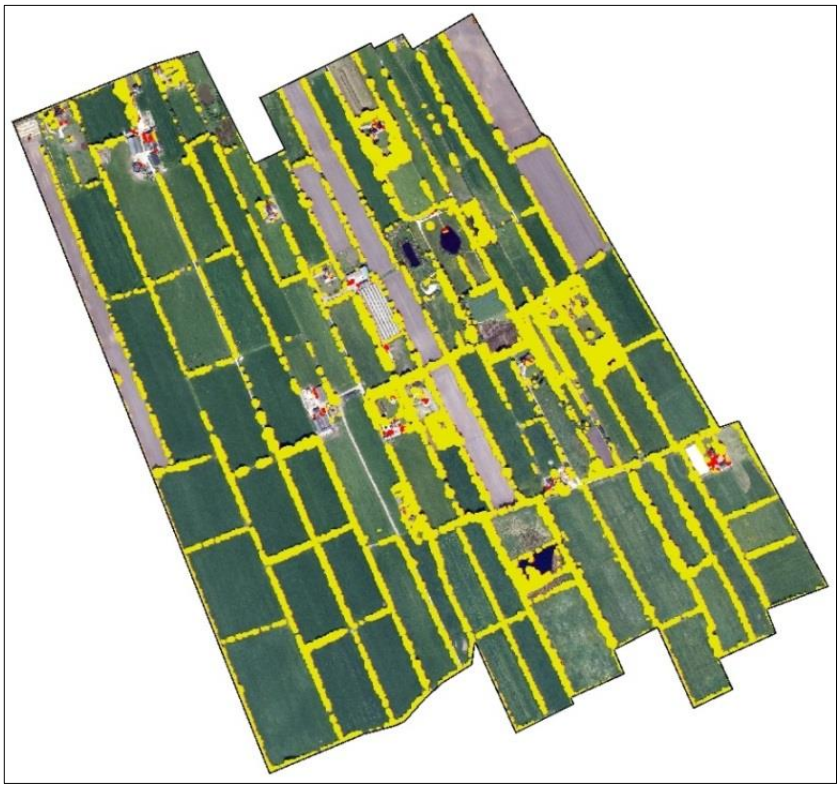

Figure 61: Unclassified vegetation dataset, created without NDVI filter

With the help of the NDVI filter, the misclassified points could be removed from the vegetation dataset as can be seen in Figure 62, where a part of the study area, containing misclassified points, is enlarged. In Figure 62, it is shown that the non-vegetation points that were misclassified as vegetation points, visible as red dots in the left image, have disappeared from the right image after applying an NDVI filter.

Figure 62: Part of the study area where NDVI (right image) is applied to remove misclassified non-vegetation points (red dots in left image)

The final vegetation dataset is shown in Figure 63. Vegetation points are displayed in yellow.

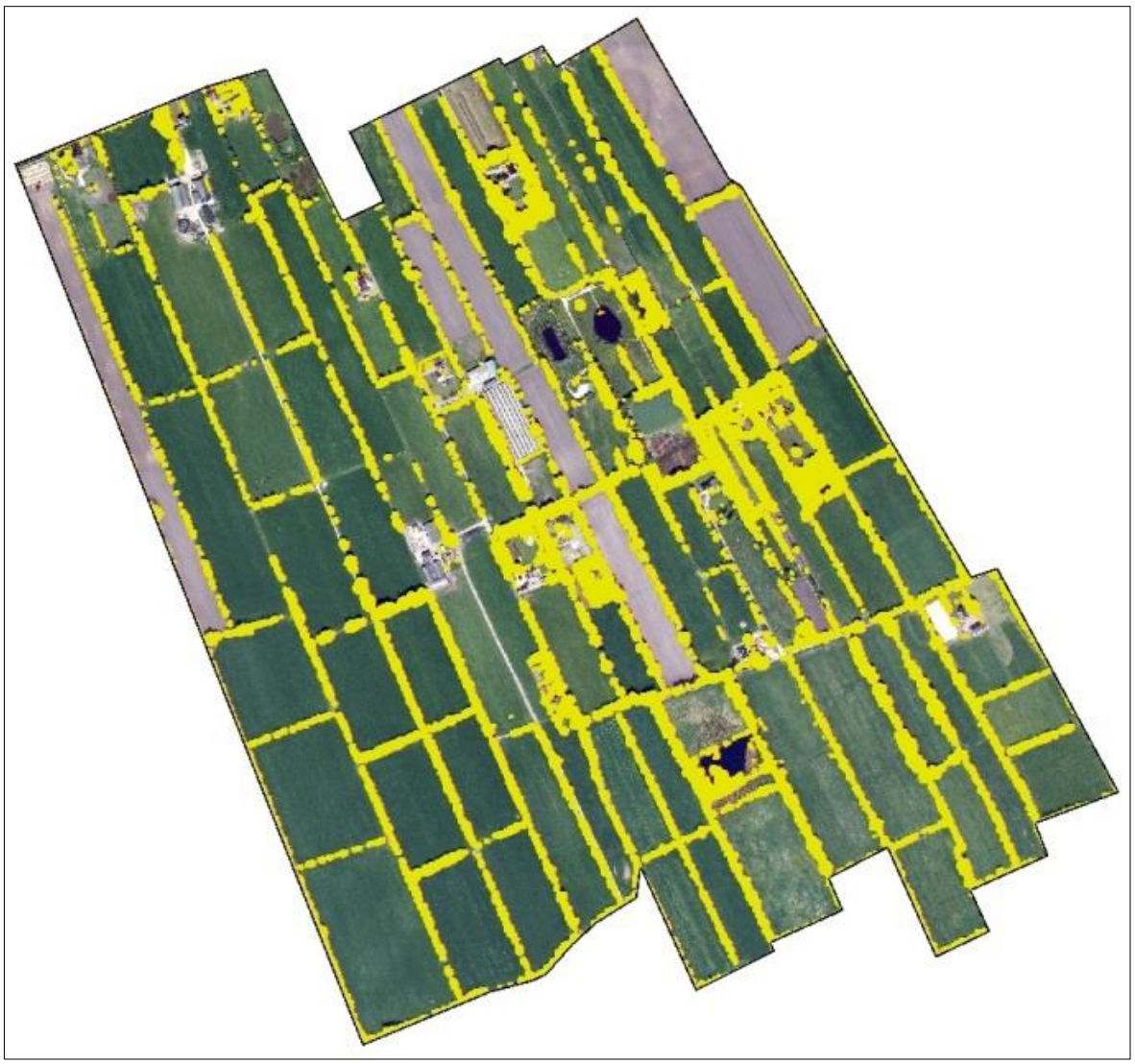

Figure 63: Unclassified vegetation dataset, created with NDVI filter

3.3.2 Statistical analysis of the LiDAR point cloud dataset

Maximum height, mean height, median height, variance, standard deviation, standard error, skewness and kurtosis were calculated and analysed to see if there were significant differences between the small green landscape elements that could be used for classification. The results are shown in the graphs in Figure 64.

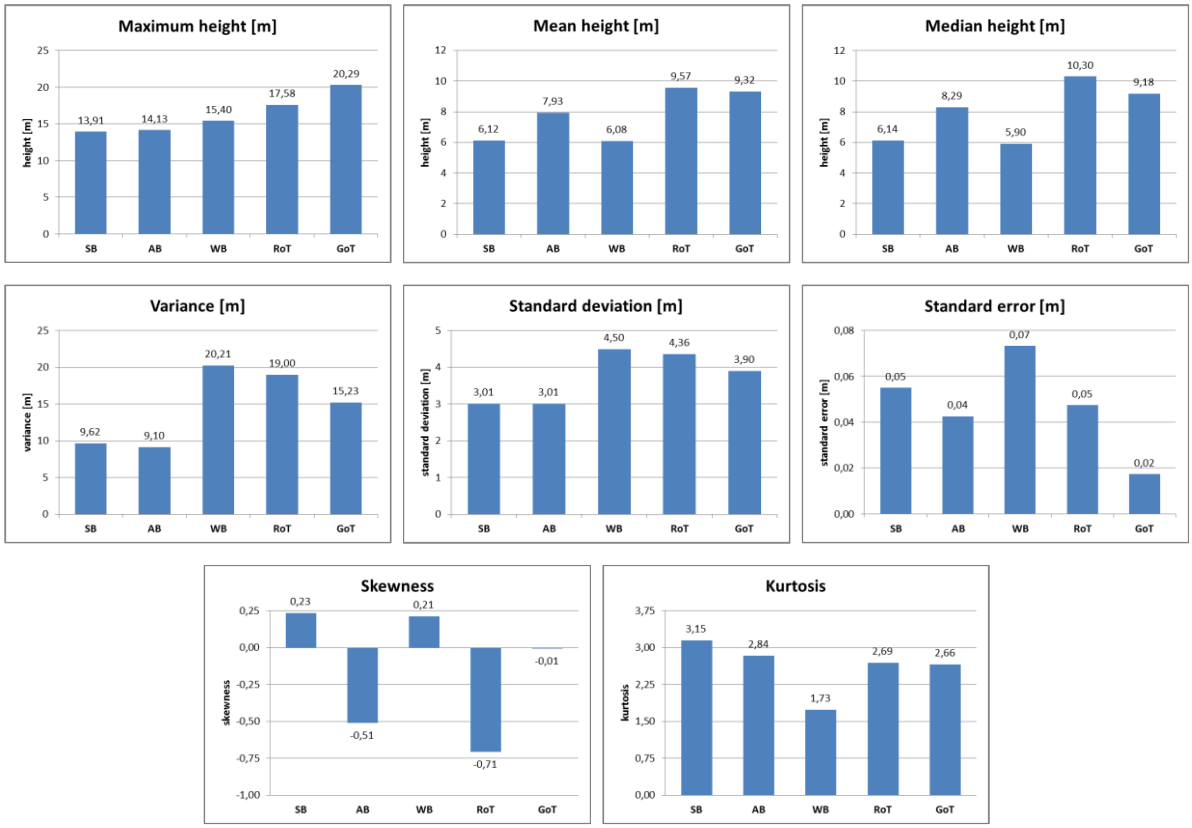

Figure 64: Graphical results of the statistical analysis

From the graphs in Figure 64, it is shown that skewness gives the most variable results, since it is the only parameter that contains both positive and negative values.

Skewness is a measure of symmetry of a point cloud distribution. When skewness is equal to zero, symmetry occurs and the point cloud has a normal distribution. However, when skewness is negative the point cloud is skewed to the left and when skewness is positive the point cloud is skewed to the right (NIST/SEMATECH, 2012; Figure 65). Skewness is negative for alder belts and rows of trees and positive for shelterbelts

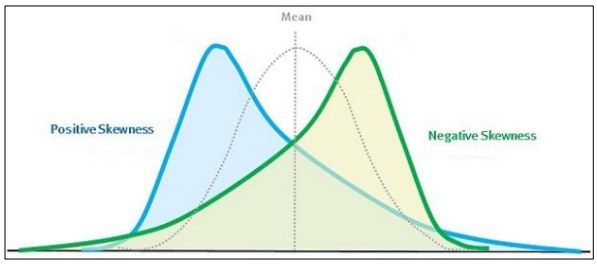

Figure 65: Skewness graph (source: http://www.assetinsights.net/Glossary/G_Skewness.html)

and wooded banks. For groups of trees, the skewness is almost equal to zero, indicating that the point cloud has a normal distribution. The highest value is found for shelterbelts, whereas the lowest value is found for rows of trees.

The left sided skewness for alder belts and rows of trees is also shown by the fact that the mean height of these small green landscape elements is lower than their median height.

Point cloud distributions are skewed to the left when more data points occur in the higher regions than in the lower regions of the distribution. For alder belts and rows of trees this is true since they do not have a shrub layer and most LiDAR points are therefore found at tree crown height. Wooded banks, shelterbelts and groups of trees can have shrub layers, but they can also be absent. Since the skewness values for wooded banks and shelterbelts are positive, more data points occur in the lower regions than in the higher regions of the distribution, indicating the presence of more shrub layers than tree crowns. Since the highest values are found for shelterbelts, it is likely that these small green landscape elements contain the most shrubs. For groups of trees, where the skewness shows a normal distribution, there is a balance between the presence of shrub layers and tree crowns.

Kurtosis is a measure that indicates if a point cloud distribution is peaked (leptokurtic) or flat (platykurtic) relative to a normal distribution. For a normal point cloud distribution, the kurtosis value is three. Point clouds with a kurtosis higher than three have a leptokurtic distribution whereas point clouds with a kurtosis lower than three have a platykurtic distribution (NIST/SEMATECH, 2012; Figure 66).

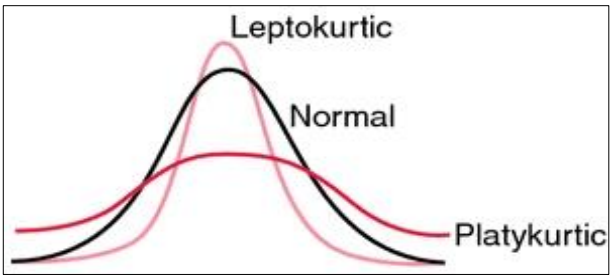

Figure 66: Kurtosis graph (source: http://medical-dictionary.thefreedictionary.com/kurtosis)

The kurtosis is only leptokurtic for shelterbelts. The lowest value is found for wooded banks.

When looking at the variance and standard deviation, it is shown that although the values of shelterbelts and alder belts do not differ significantly among each other they are both lower than the values of the other small green landscape elements. Shelterbelts and alder belts both have a variance lower than 10 and a standard deviation almost equal to three, whereas the other small green landscape elements have higher values, indicating that shelterbelts and alder belts have a less deviating point cloud distribution than the other small green landscape elements.

Groups of trees have the highest maximum height, whereas shelterbelts and alder belts have the lowest maximum height. Mean and median height, however, is highest for rows of trees, indicating that the proportion of high trees within the rows of trees is higher than the proportion of high trees within the groups of trees.

3.3.3 Classifying the small green landscape elements (step 2)

In the second modelling step, small green landscape elements were classified from the unclassified LiDAR point cloud vegetation dataset that was created in the first step. First, maximum height, mean height, standard deviation, kurtosis and skewness were calculated with the help of the *lascanopy* tool. In Figure 67, the calculation results are shown. Figure 67 shows that approximately half of the small green landscape elements have a maximum height of more than 15 m, a mean height of more than 7,0 m and a skewness higher than zero. On the other hand, only three small green landscape elements have a standard deviation of more than 3,0 m and only three small green landscape elements have a kurtosis higher than three.

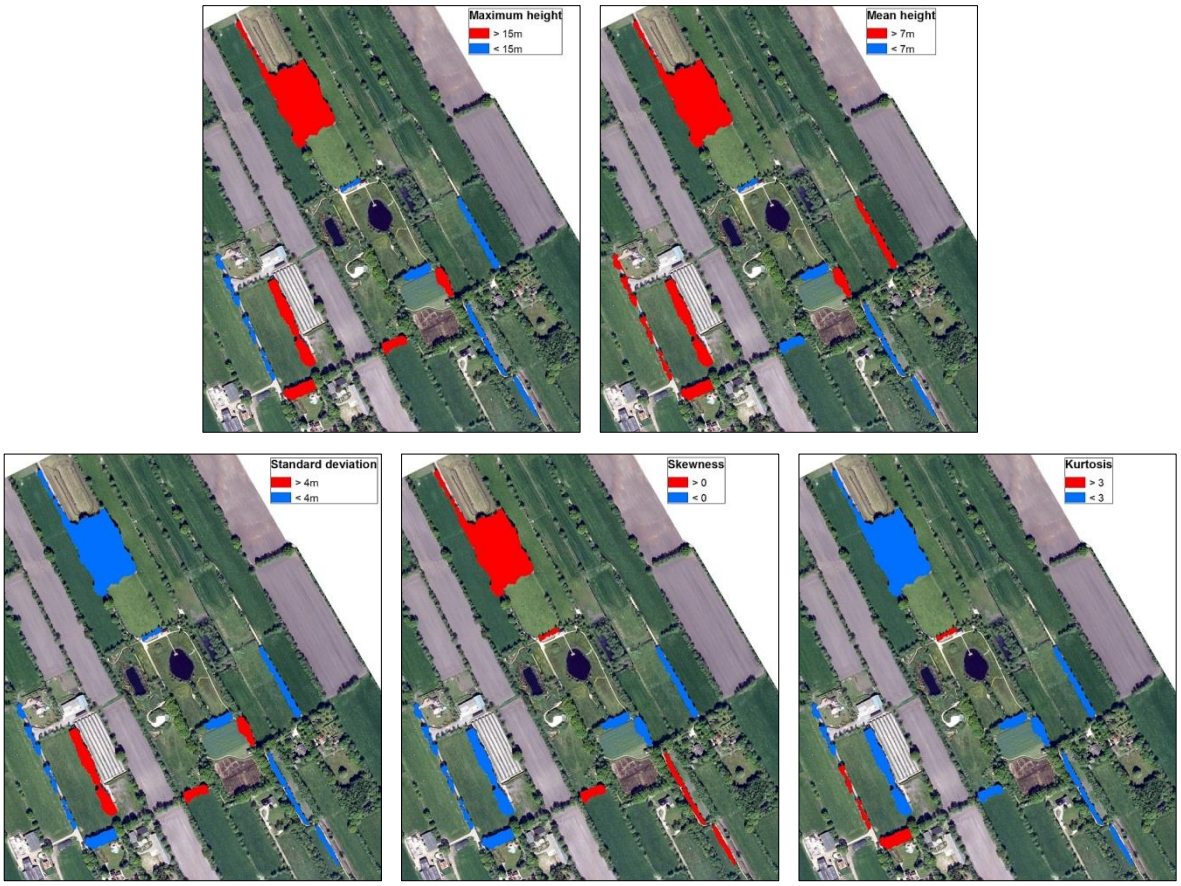

Figure 67: Overview of statistical results as calculated with the *LAScanopy* tool

After calculation of the statistics, small green landscape elements were classified based on the selection criteria as mentioned in Table 1 (see Chapter 2.5.3). In Figure 68, the classification results are shown. Figure 68 shows that one wooded bank, two rows of trees, one shelterbelt, two alder belts were classified from the LiDAR point cloud vegetation dataset, whereas seven small green landscape elements could not be identified and classified at all. From the classified small green landscape elements, only the shelterbelt, one row of trees, one complete alder belt and one half of an alder belt were classified correctly.

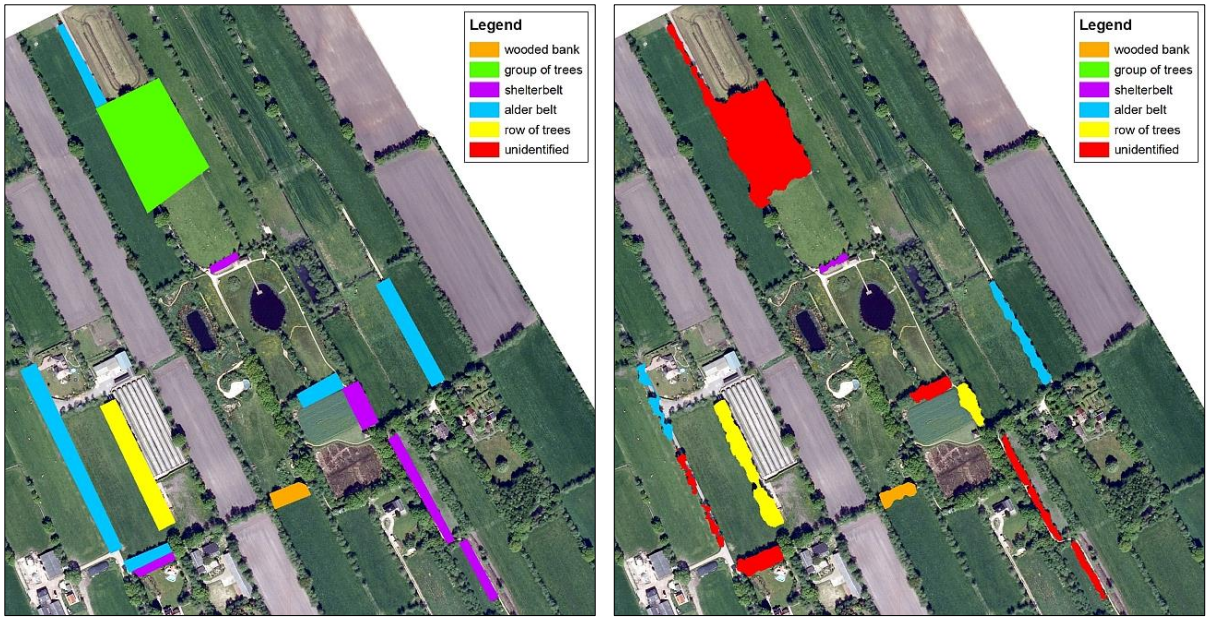

Figure 68: Result of the classification of small green landscape elements with the data processing model (right image) and an overview of the small green element types as identified during the field inventory (left image)

3.3.4 Discussion

No problems occurred during the pre-processing phase and first step of modelling. Carrying out the second step, however, resulted in poor classification results, as was shown in the previous paragraph (Figure 68). Several factors might have caused these poor classification results.

First of all, some of the boundaries of the small green landscape elements created during modelling were not similar to the boundaries of the small green landscape elements as determined during the field inventory. In Figure 69, it is shown that at two locations the model merged boundaries of two different small green landscape elements into one boundary (top left image and bottom left image) whereas at one location the boundary of one small green landscape element was separated into four smaller boundaries (right image).

Figure 69: Vegetation boundary problems that occurred during modelling (purple boundary = boundary determined in the field, yellow boundary = boundary created by the *lasboundary* tool)

Merging and separating of vegetation boundaries is caused by the position of tree crowns. When tree crowns are close together and fuse, the *lasboundary* tool will see them as one vegetation element and merging will take place. On the other hand, when tree crowns are further away from each other and do not fuse, the *lasboundary* tool will see them as different vegetation elements and separating will take place. To create the best fitting boundaries, it is important to determine the right value for the concavity parameter. Concavity is the distance between break points that represent the course of a boundary. In this research, a concavity of 4,0 was used, because although increasing or decreasing the value did solve the problems at the locations discussed from Figure 69, even more problems were caused at other locations. A concavity of 4,0 was therefore seen as the best fitting concavity value in this research.

Another factor that might have caused poor classification results is the fact that average values of the different shelterbelts and average values of the different alder belts were used for the statistical analysis. By using average values, significant differences that might occur amongst the shelterbelts or amongst the alder belts are not taken into account. The boxplots in Figure 70 show that there are

indeed differences amongst the shelterbelts and amongst the alder belts. The boxplots of the shelterbelts show the highest differences, in relation to shelterbelt 3 (SB3) and shelterbelt 9 (SB9) that both have a higher median height and maximum height than the other shelterbelts. Although the differences amongst the alder belts are less evident than the differences amongst the shelterbelts, the boxplots in Figure 70 do show that median height and maximum height of alder belt 7 (AB7) are higher than median height and maximum height of the other alder belts.

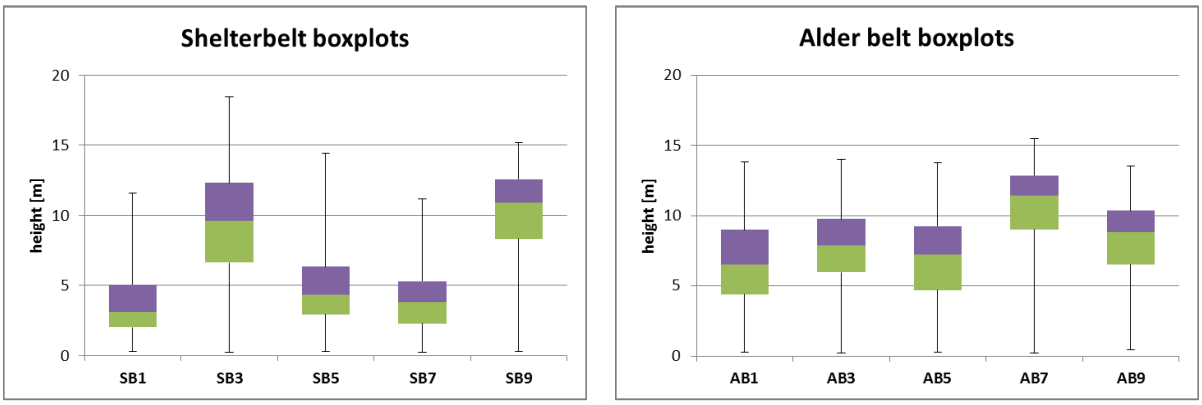

Figure 70: Boxplots of shelterbelts and alder belts

To find out if the differences between the belts that are shown in Figure 70 are significant, a significance test was carried out. Since more than two small green landscape elements needed to be compared with each other and since the point clouds of none of these landscape elements showed a normal distribution (see Appendix 3 for an overview of their normability plots), the Kruskal-Wallis test was used. The Kruskal-Wallis test is a non-parametric test, based on ranking, which can be used when samples are not normally distributed or when more than two samples need to be compared with each other. The test does not show WHICH samples are significant different, but IF one or more samples are significant different. A significant difference exists if a calculated *p*-value is lower than a predefined significance level (α). Results of the Kruskal-Wallis, shown in Table 4 for shelterbelts and Table 5 for alder belts, show that in both cases $p < \alpha$, and therefore it can be concluded that at least one shelterbelt and one alder belt differ significantly from the other belts of the same type.

Table 4: Results of the Kruskal-Wallis significance test for shelterbelts

shelterbelt number	N	rank sum (R)	R^2/N		
SB1	687	3,541E+06	1,825E+10		
SB3	8673	1,147E+08	1,516E+12	**H**	7982,65
SB5	6115	4,022E+07	2,646E+11	**df**	4
SB7	2362	1,295E+07	7,101E+10	**p**	0,00
SB9	2657	3,863E+07	5,616E+11	**α**	0,05
total	**20494**		**2,432E+12**	**significant difference**	yes

Table 5: Results of the Kruskal-Wallis significance test for alder belts

alder belt number	N	rank sum (R)	R^2/N		
AB1	5149	6,165E+07	7,381E+11		
AB3	13471	2,004E+08	2,982E+12	**H**	4293,66
AB5	4900	6,197E+07	7,836E+11	**df**	4
AB7	3610	8,424E+07	1,966E+12	**p**	0,00
AB9	3245	5,305E+07	8,673E+11	**α**	0,05
total	**20494**		**7,337E+12**	**significant difference**	yes

In Appendix 4, the statistical calculation results for each shelterbelt and alder belt are compared with the selection criteria that are used for the classification of the small green landscape elements. The results are summarized in Table 6.

Table 6: Comparison of statistical calculation results with the selection criteria for the classification of small green landscape elements for shelterbelts and alder belts

statistical type	selection criteria	higher than selection criteria	lower than selection criteria
maximum height	< 15	SB3 ; SB9	SB1 ; SB5 ; SB7
mean height	< 7	SB5 ; SB9	SB1 ; SB3 ; SB7
standard deviation	< 4	SB5	SB1 ; SB3 ; SB7 ; SB9
skewness	≥ 0	SB1 ; SB5 ; SB7	SB3 ; SB9
kurtosis	≥ 3	SB1 ; SB9	SB3 ; SB5 ; SB7
maximum height	< 15	AB7	AB1 ; AB3 ; AB5 ; AB9
mean height	≥ 7	AB5 ; AB7 ; AB9	AB1 ; AB3
standard deviation	< 4		AB1 ; AB3 ; AB5 ; AB7 ; AB9
skewness	< 0	AB1	AB3 ; AB5 ; AB7 ; AB9
kurtosis	< 3	AB7	AB1 ; AB3 ; AB5 ; AB9

In Table 6, it is shown that in three cases, displayed in the red boxes, shelterbelt 3 (SB3), shelterbelt 5 (SB5) and shelterbelt 9 (SB9) do not satisfy the selection criteria for small green landscape element classification, while in one case, shelterbelt 7 (SB7) does not satisfy these selection criteria. Since the boxplots in Figure 70 have already shown that shelterbelt 3 and shelterbelt 9 differ from the other shelterbelts, it is likely that these two shelterbelts are the ones that are significant different from the rest and removing them from the training dataset might increase classification results.

In case of the alder belts, Table 6 shows that in three cases, displayed in the purple boxes, alder belt 7 (AB7) does not satisfy the selection criteria for small green landscape element classification whereas in one case, alder belt 1 (AB1), alder belt 5 (AB5) and alder belt 9 (AB9) do not satisfy these selection criteria. Since the boxplots in Figure 70 have already shown that alder belt 7 differs from the other alder belts, it is likely that this alder belt is the one that is significant different from the rest and removing this alder belt from the training dataset might increase classification results.

3.4 Validating the data processing model

Despite the poor classification results of the training data, it was still decided to run the data processing model for the whole study area. Expectations were not high and, as the classification results in Figure 71 show, classification indeed ended up in poor results again. Except for two small green landscape elements in the northern part of the study area, none of the small green landscape elements were classified as shelterbelt, whereas some small green landscape elements were classified as alder belt or as group of trees. Most small green landscape elements, however, were not identified and classified at all. Since the study area is known for the presence of shelterbelts, it is strange that almost none of the small green landscape elements were classified as shelterbelt.

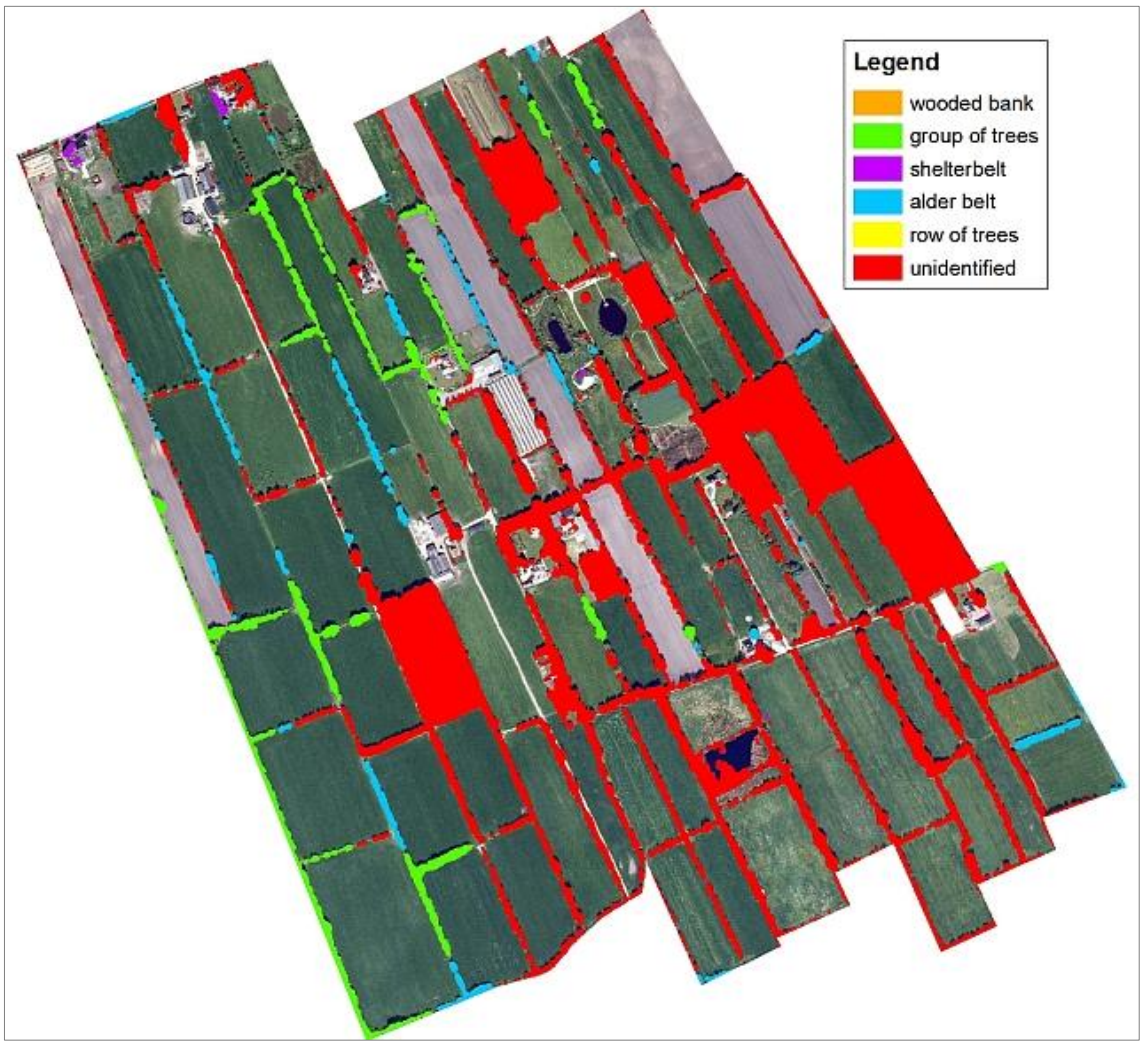

Figure 71: Classification results for the whole study area after running the data processing model

When looking at the classification results for the validation data (Figure 72), results were poor again. Seventeen small green landscape elements were identified. From these 17 small green landscape elements, ten elements were not classified at all. From the other seven elements, two elements were classified as group of trees, four elements were classified as alder belt and one element was classified as row of trees. From the seven classified elements, only two alder belts were classified

correctly. The results are shown in Table 7. Since classification results were so poor, carrying out an accuracy assessment would be useless and it was therefore decided to skip this last assessment step.

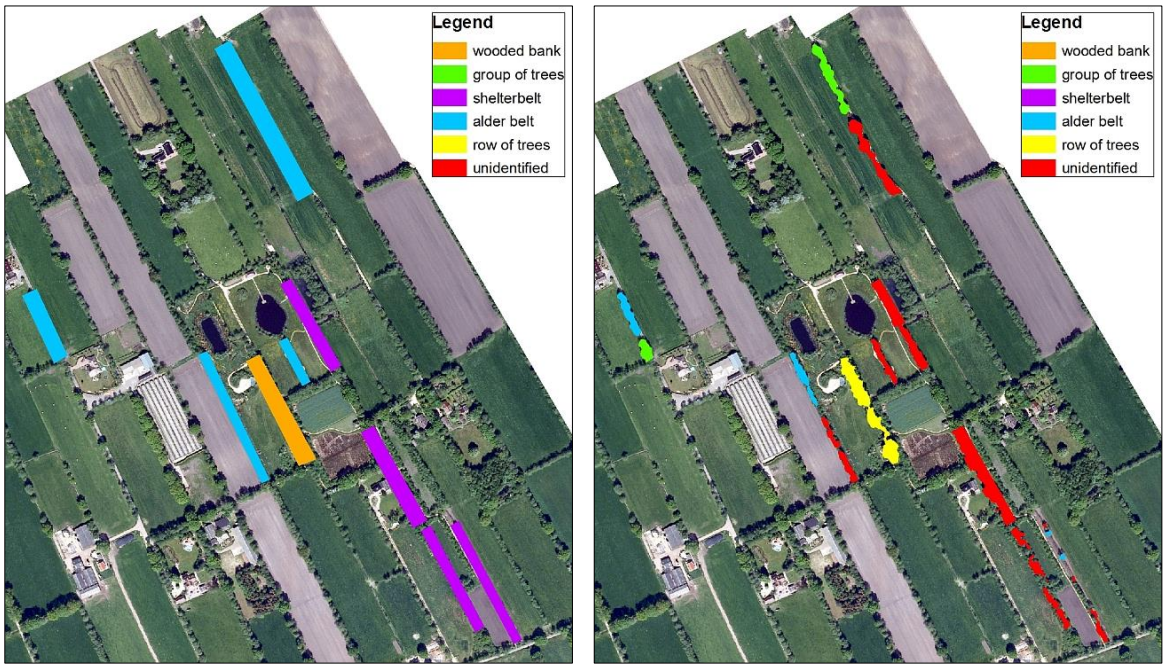

Figure 72: Classification results for the validation data after running the data processing model (right image) and an overview of the small green element types as identified during the field inventory (left image)

Table 7: Comparison between field inventory results and classification results of the small green landscape elements for the validation data

SGLE	results field inventory	results classification	SGLE	results field inventory	results classification
1	AB	GOT	10	SB	U
2	AB	U	11	SB	U
3	AB	AB	12	SB	U
4	AB	GOT	13	SB	AB
5	SB	U	14	SB	AB
6	AB	U	15	SB	U
7	WB	ROT	16	SB	U
8	AB	AB	17	SB	U
9	AB	U			

4 Conclusions and recommendations

In this thesis research, it was examined if a data processing model could be created for the classification of small green landscape elements from unclassified point cloud LiDAR data. A statistical approach was used to define selection criteria for the classification and LAStools in combination with ArcGIS was used for modelling. Although the results from the pre-processing phase and the first phase of modelling, extracting vegetation from an unclassified point cloud LiDAR dataset were good, the last phase of modelling, classifying small green landscape elements, only gave poor results, both during calibration and validation. It can therefore be questioned if the data processing model that was created in this thesis research is useful for small green landscape element classification.

However, it should be taken into account that because of inaccessibility of a large part of the study area, only 26 small green landscape elements could be identified and used for calibration and validation. Since this amount is far below the advised amount of samples that should be used for calibration and validation it could have affected both statistical analysis and classification in a negative way, leading to unreliable classification results.

It is therefore recommended to calibrate and validate the data processing model in another study area, where it is possible to collect a sufficient amount of samples that can be used for calibration and validation. At least 30 samples for each map class should be collected, but an amount of 50 samples is even better. When classification still gives poor results, small green landscape elements that show significant differences compared to other small green landscape elements could be removed from the statistical analysis dataset to see if classification results improve.

Furthermore, the data processing model can be extended with other selection criteria that are not based on statistical analysis. For example, wooded banks are always situated on a wall of earth. A wall of earth should be visible in a Digital Elevation Model (DEM) and including a DEM in the classification tree might therefore improve classification results.

When recommendations are carried out, the data processing model might give better classification results, although it is expected that a 100 per cent correct classification will never occur. However, some of the small green element types might be classified correctly, so that field inventories for these small green element types are no longer needed and subsidy applications for the Agricultural Nature and Landscape Management system will at least partly be accelerated and simplified.

References

Andújar D., Escolà A., Rosell-Polo J.R., Fernández-Quintanilla C. and Dorado J. (2013). Potential of a terrestrial LiDAR-based system to characterise weed vegetation in maize crops. *Computers and electronics in agriculture*, vol.92, p.11-15

Calders K. (2015). *Terrestrial laser scanning for forest monitoring*. PhD thesis, Wageningen University

Chen Q. (2007). Airborne lidar data processing and information extraction. *Photogrammetric engineering & remote sensing*, February 2007, p.109-112

Claessens H., Oosterbaan A., Savill P. and Rondeux J. (2010). A review of the characteristics of black alder (Alnus glutinosa (L.) Gaertn.) and their implications for silvicultural practices. *Forestry*, vol.83, no.2, p.163-175

Congalton R.G. (2001). Accuracy assessment and validation of remotely sensed and other spatial information. *International journal of wildland fire*, vol.10, p.321-328

Doane D.P and Seward L.E. (2011). Measuring skewness: a forgotten statistic? *Journal of Statistics Education*, vol.19, no.2, p.1-18

Estornell J., Angel Ruiz L. and Velázquez-Marti B. (2011). Study of shrub cover and height using LIDAR data in a Mediterranean area. *Forest sciences*, vol.57, no.3, p.171-179

Faridhouseini A., Mianabadi A., Bannayan M. and Alizadeh A. (2011). Lidar remote sensing for forestry and terrestrial applications. *International journal of applied environmental sciences*, vol.6, no.1, p.99-114

Ferraz A., Bretar F., Jacquemoud S., Gonçalves G., Pereira L., Tomé M. and Soares P. (2012). 3-D mapping of a multi-layered Mediterranean forest using ALS data. *Remote sensing of environment*, vol.121, p.210-223

Ficetola G.F., Bonardi A., Mücher C.A., Gilissen N.L.M. and Padoa-Schioppa E. (2014). How many predictors in species distribution models at the landscape scale? Land use versus LiDAR-derived canopy height. *International journal of geographical information science*, vol.28, no.8, p.1723-1739

Geerling G.W., Labrador-Garcia M., Clevers J.G.P.W., Ragas A.M.J. and Smits A.J.M. (2007). Classification of floodplain vegetation by data fusion of spectral (CASI) and LiDAR data. *International journal of remote sensing*, vol.28, no.19, p.4263-4284

Geertsema W., Griffioen A., Meeuwsen H.A.M. and Kalkhoven J.T.R. (2003). *Natuur en identiteit, een rapport over 2002: groenblauwe dooradering is belangrijk voor natuur en identiteit in het*

agrarisch cultuurlandschap. Wageningen, Alterra Wageningen UR (University & Research centre). Alterra rapport 712

Grashof-Bokdam C.J., Akkermans L.M.W., Meeuwsen H.A.M., van der Veen M. and Vos C.C. (2009). *Synergie: de meerwaarde van het combineren van bos en opgaande dooradering voor biodiversiteit*. Wageningen, Alterra Wageningen UR (University & Research centre). Alterra rapport 1854

Gwenzi D. and Lefsky M.A. (2014). Modeling canopy height in a savannah ecosystem using spaceborne lidar waveforms. *Remote sensing of environment*, vol.154, p.338-344

Hammers M., Sierdsema H., van Heusden W.R.M. and Melman Th.C.P. (2014). *Nieuw stelsel agrarisch natuurbeheer, voortgang ontwikkeling beoordelingssystematiek*. Wageningen, Alterra Wageningen UR (University & Research centre). Alterra rapport 2561

Hantson W., Kooistra L. and Slim P.A. (2012). Mapping invasive woody species in coastal dunes in the Netherlands: a remote sensing approach using LIDAR and high-resolution aerial photographs. *Applied vegetation science*, vol.15, p.536-547

Höfle B. (2014). Radiometric correction of terrestrial LiDAR point cloud data for individual maize plant detection. *IEEE geoscience and remote sensing letters*, vol.11, no.1, p.94-98

Index Natuur en Landschap, onderdeel Landschapsbeheertypen, version 2015. Downloaded from: http://www.portaalnatuurenlandschap.nl/assets/Index-Landschap-beheerjaar-2015-def-versie-voor-PNL.pdf (09.12.2014)

Koomen A.J.M., Maas G.J. and Weijschede T.J. (2007). *Veranderingen in lijnvormige cultuurhistorische landschapselementen, resultaten van een steekproef over de periode 1900-2003*. Wageningen, wettelijke onderzoekstaken natuur & milieu. WOt-Rapport 34

Leusink ir. J.G. and Dijkman ir. S (2010). *Finale rapportage AHN2-2009 perceel 1, eindlevering, versie 1*. Utrecht, 6 juli 2010

Lillesand T.M., Kiefer R.W. and Chipman J.W. (2008). *Remote sensing and image interpretation*. Sixth edition. John Wiley & Sons, Inc

Liu J., Shen J., Zhao R. and Xu S. (2013). Extraction of individual tree crowns from airborne LiDAR data in human settlements. *Mathematical and computer modelling*, vol.58, p.524-535

McGaughey R.J. (2014). *FUSION/LLDV: software for LIDAR data analysis and visualization – version 3.42*. United States Department of Agriculture, Forest Service

Melman Th.C.P., Hammers M., Clement J. and Schmidt A.M. (2014). *Ontwerp beoordelingskader nieuwe stelsel agrarisch natuurbeheer*. Wageningen, Alterra Wageningen UR (University & Research centre). Alterra rapport 2503

Mücher C.A., Roupioz L., Kramer H., Bogers M.M.B., Jongman R.H.G., Lucas R.M., Kosmidou V.E., Petrou Z., Manakos I., Padoa-Schioppa E., Adamo M. and Blonda P. (2014). Synergy of airborne LiDAR and Worldview-2 satellite imagery for land cover and habitat mapping: a BIO_SOS_EODHaM case study for the Netherlands. *International journal of applied earth observation and geoinformation*. Article in press

Mulders A. (2014). *Hoofdstructuur vernieuwd stelsel Agrarisch Natuur- en Landschapsbeheer, versie 5.0*. Agrarisch natuur- en landschapsbeheer 2016

Natuurbeheerplan Groningen (2015). Downloaded from: http://www.provinciegroningen.nl/fileadmin/user_upload/Documenten/Downloads/Natuurbeheerplan_2015_provincie_Groningen.pdf (5.12.2014)

Nex F. and Rinaudo F. (2011). LiDAR or photogrammetry? Integration is the answer. *Rivista Italiana di telerilevamento*, vol.43, no.2, p.107-121

Nieuwenhuizen W., Daamen W.P., van Egmond P.M., Gerritsen A.L., Kersten P.H., Kistenkas F.H., Pedroli G.B.M., Roos-Klein Lankhorst J., Schöne M.B. and Schröder R.R.G. (2008). *Landschap in de natuurbalans 2007: hoe staan de rijksdoelen voor het landschap er voor?* Bilthoven, Planbureau voor de Leefomgeving (PBL). PBL-publicatienummer 500402010

NIST/SEMATECH (2012). E-Handbook of statistical methods, http://www.itl.nist.gov/div898/handbook/eda/section3/eda35b.htm (16.07.2015)

Petrie G. and Toth C.K. (2009). Introduction to laser ranging, profiling, and scanning. In: *Topographic laser ranging and scanning – principles and processing*. Shan J. and Toth C.K. (eds). Taylor and Francis Group, Boca Raton, Florida

Reutebuch S.E., Andersen H.E. and McGaughey R.J. (2005). Light detection and ranging (LIDAR): an emerging tool for multiple resource inventory. *Journal of forestry*, September 2005, p.286-292

Shafri H.Z.M., Ismail M.H., Razi M.K.M., Anuar M.I. and Ahmad A.R. (2012). Application of LiDAR and optical data for oil palm plantation management in Malaysia. In: *SPIE Asia-Pacific remote sensing*. International society for optics and photonics. p.852608 1-14

Smits M.J.W. and van Alebeek F.A.N. (2007). *Biodiversiteit en kleine landschapselementen in de biologische landbouw, een literatuurstudie*. Wageningen, wettelijke onderzoekstaken natuur & milieu. WOt-rapport 39

Straatsma M., Middelkoop H., Pebesma E. and Wesseling C. (2004). Mapping of vegetation characteristics using lidar and spectral remote sensing. In: *NCR-days 2003, dealing with floods within constraints*, November 6-8. Douben N. and van Os A.G. (eds). NCR publication 23-2004, p.48-50

Ussyshkin V. and Theriault L. (2011). Airborne Lidar: advances in discrete return technology for 3D vegetation mapping. *Remote sensing*, vol.3, p.416-434

Van Der Zon N. (2013). *Kwaliteitsdocument AHN, versie 1.3*.

Verrelst J., Geerling G.W., Sykora K.V. and Clevers J.G.P.W. (2009). Mapping of aggregated floodplain plant communities using image fusion of CASI and LiDAR data. *International journal of applied earth observation and geoinformation*, vol.11, p.83-94

Ward R.D., Burnside N.G., Joyce C.B. and Sepp K. (2013). The use of medium point density LiDAR elevation data to determine plant community types in Baltic coastal wetlands. *Ecological indicators*, vol.33, p.96-104

Weis M., Andújar D., Peteinatos G.G. and Gerhards R. (2013). Improving the determination of plant characteristics by fusion of four different sensors. In: *Precision agriculture '13*. Wageningen academic publishers, the Netherlands. p.63-69

Weiss U., Biber P., Laible S., Bohlmann K. and Zell A. (2010). Plant species classification using a 3D LIDAR sensor and machine learning. In: *Machine learning and applications (ICMLA), 2010 Ninth International Conference on*. IEEE. p.339-345

Willers J.L., Wu J., O'Hara C. and Jenkins J.N. (2012). A categorical, improper probability method for combining NDVI and LiDAR elevation information for potential cotton precision agricultural applications. *Computers and electronics in agriculture*, vol.82, p.15-22

Xiao W., Xu S., Oude Elberink S. and Vosselman G. (2012). Change detection of trees in urban areas using multi-temporal airborne lidar point clouds. *SPIE proceedings, vol.8532, remote sensing of the ocean, sea ice, coastal waters, and large water regions*

Yengoh G.T., Dent D., Olsson L., Tengberg A.E. and Tucker C.J. (2014). *The use of the Normalized Difference Vegetation Index (NDVI) to assess land degradation at multiple scales: a review of the current status, future trends, and practical considerations.* Lund university centre for sustainability studies – LUCSUS, Sweden

Appendix 1 Top views* and point clouds of the 26 small green landscape elements identified during the field visit

* For visualisation of the top views, an aerial photograph of 2008 was used. The visualisations might therefore deviate from the reality.

Wooded bank 1

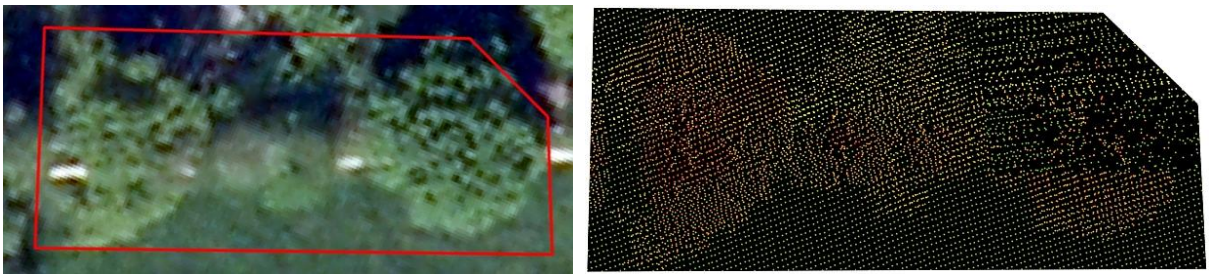

Wooded bank 2

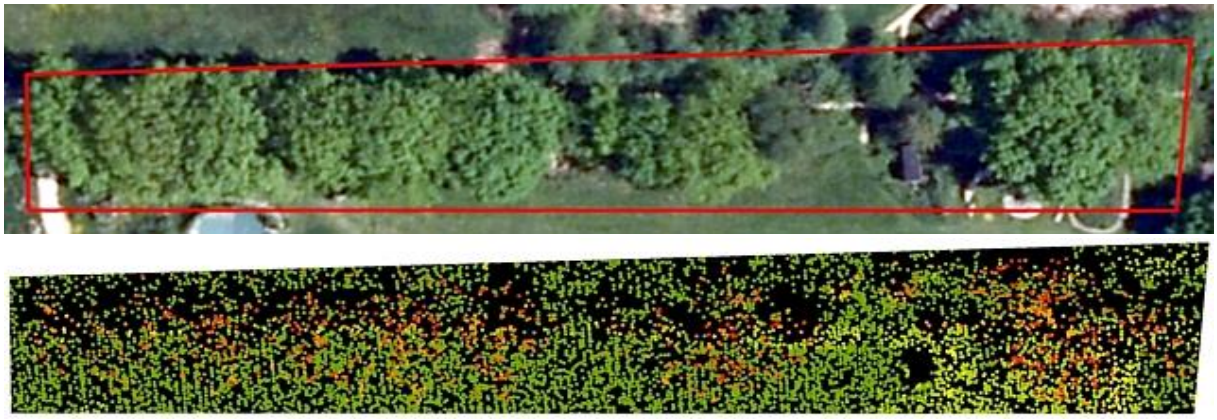

Group of trees 1

Group of trees 2

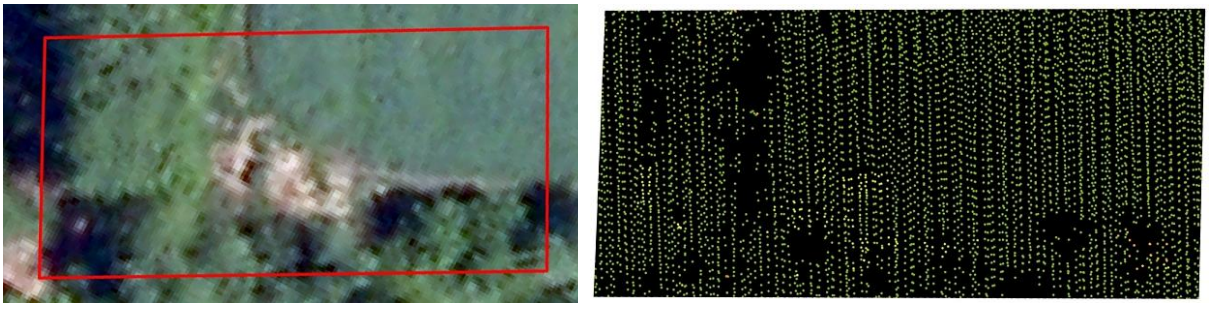

Group of trees 3

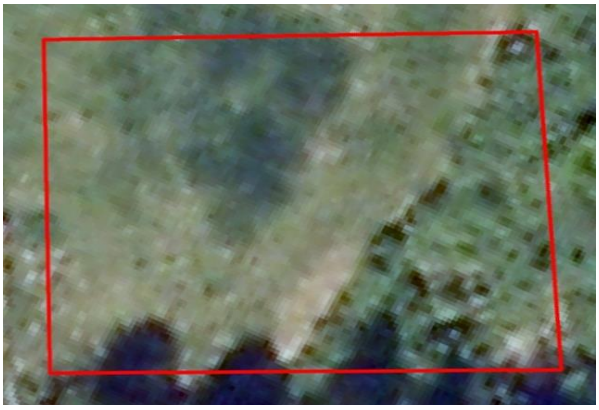

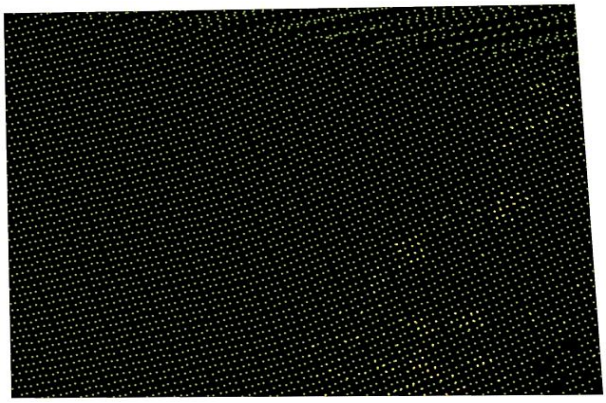

Shelterbelt 1

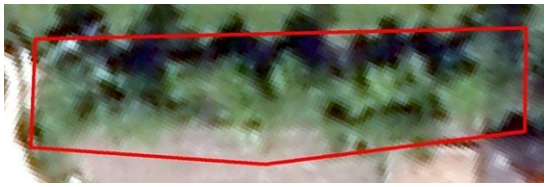

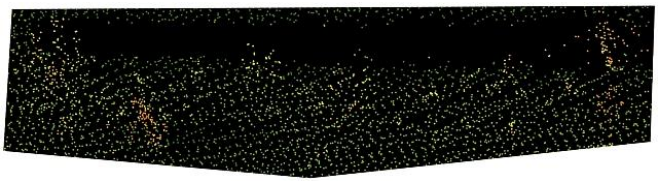

Shelterbelt 2

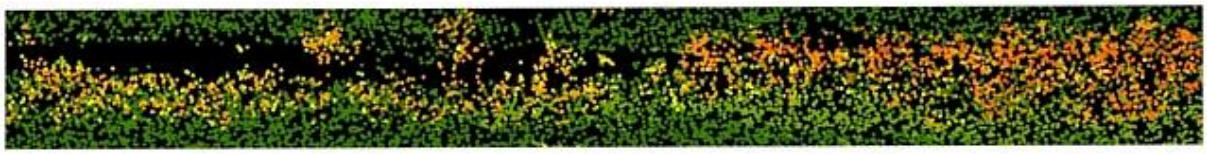

Shelterbelt 3

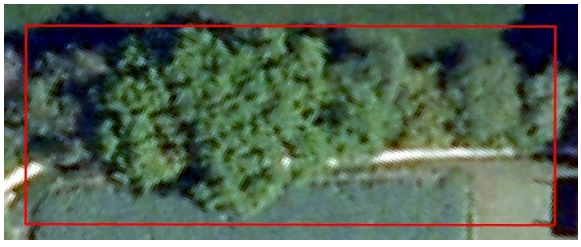

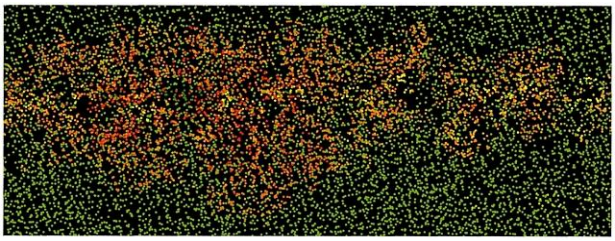

Shelterbelt 4

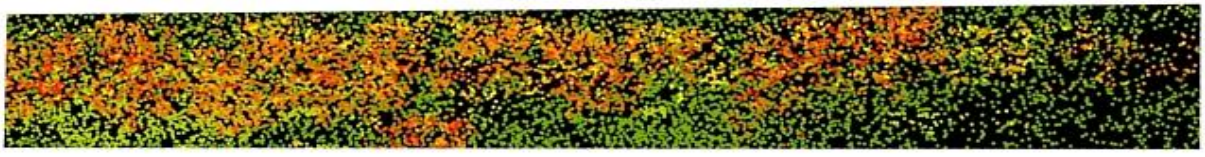

Shelterbelt 5

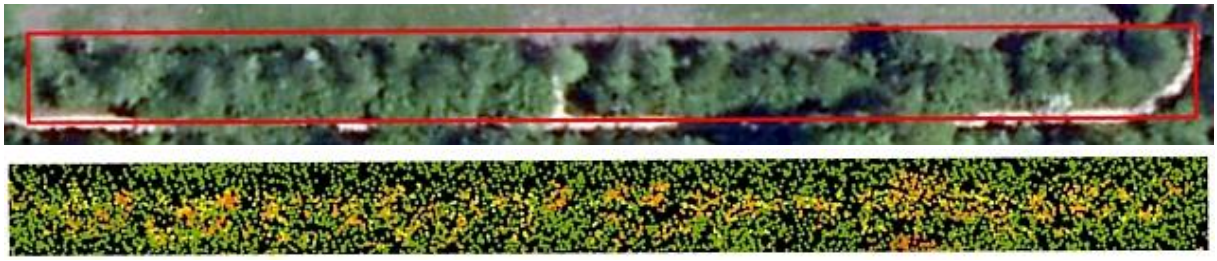

Shelterbelt 6

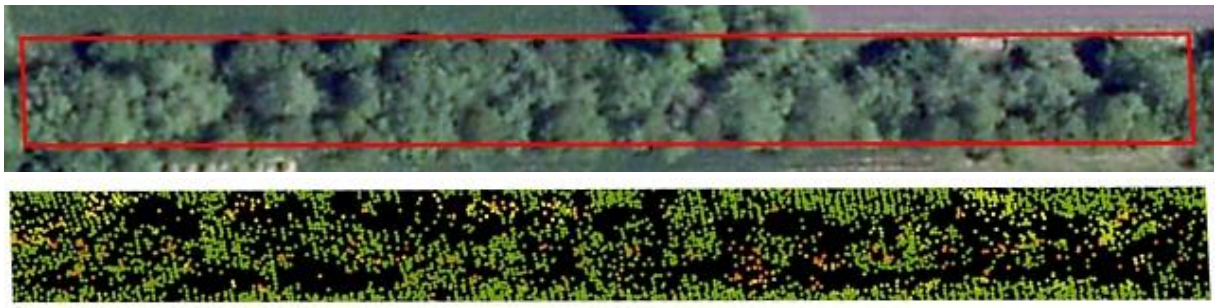

Shelterbelt 7

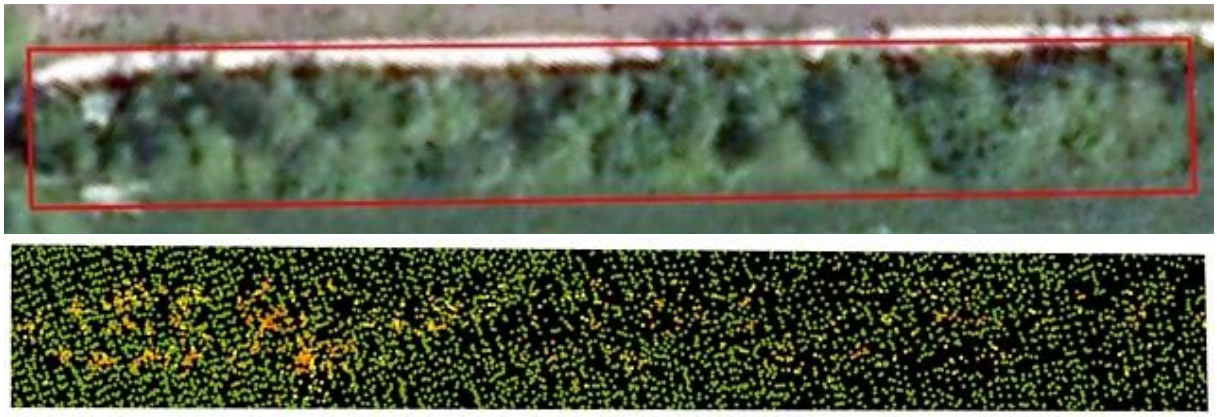

Shelterbelt 8

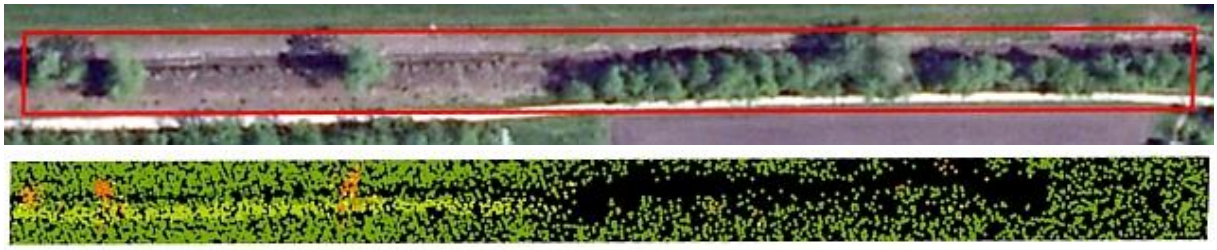

Shelterbelt 9

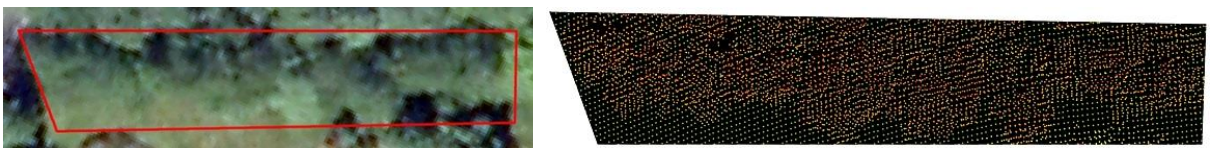

Alder belt 1

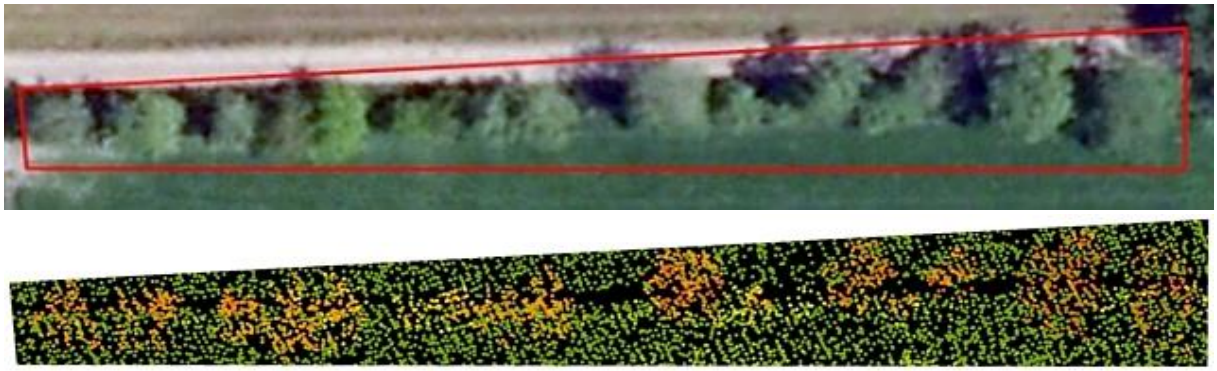

Alder belt 2

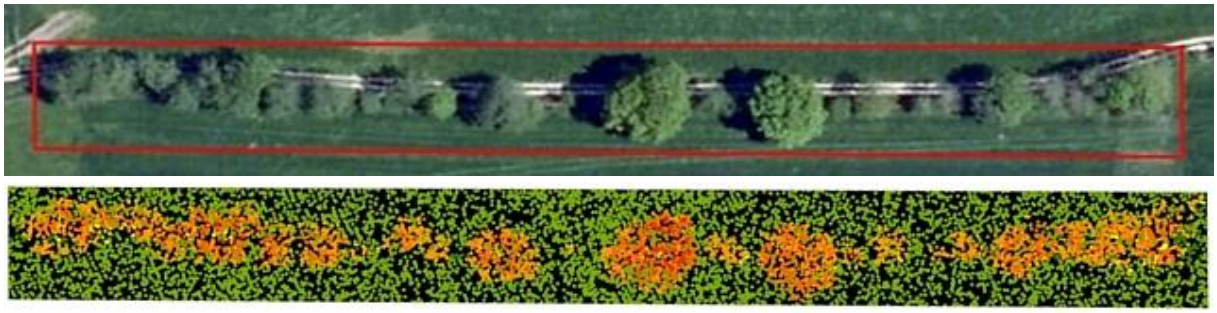

Alder belt 3

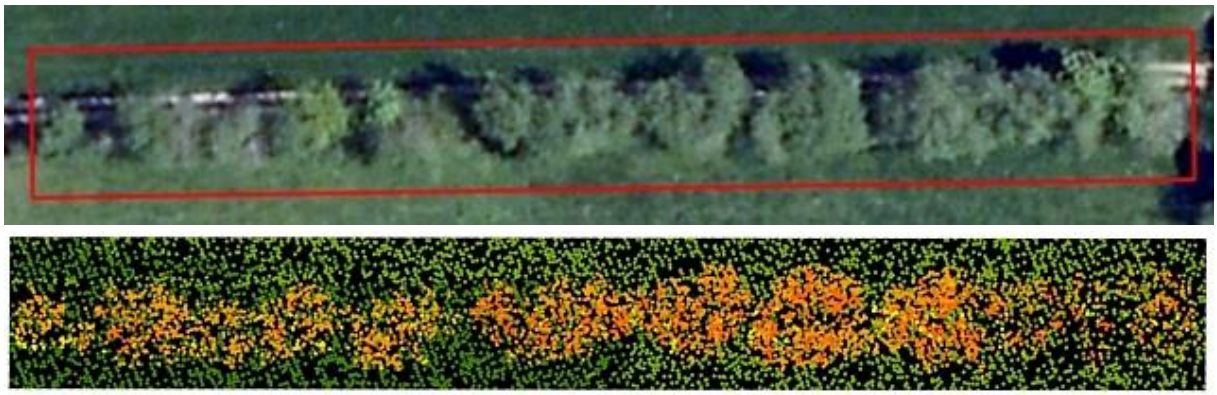

Alder belt 4

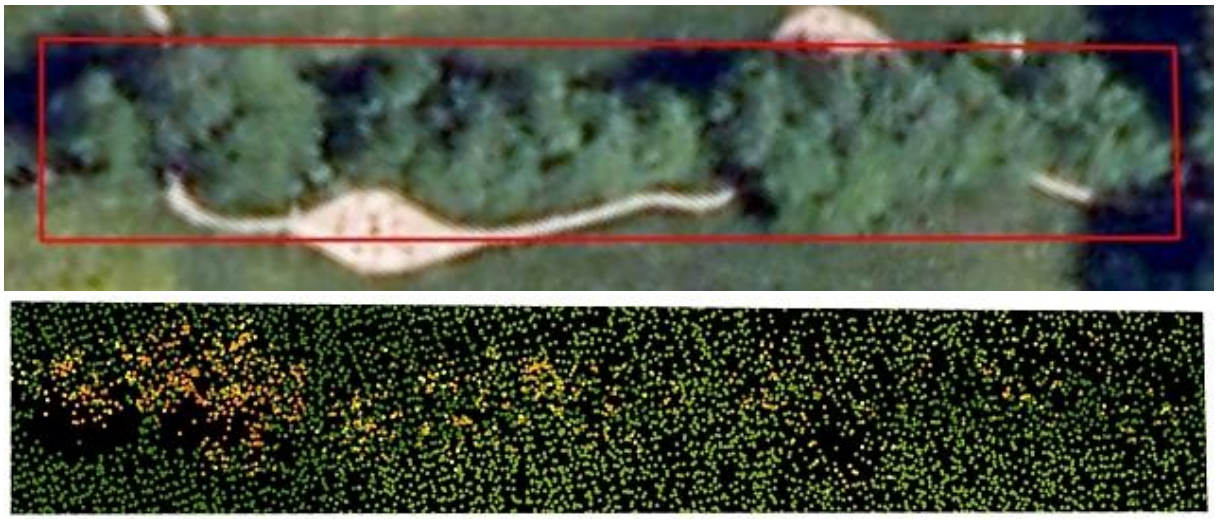

Alder belt 5

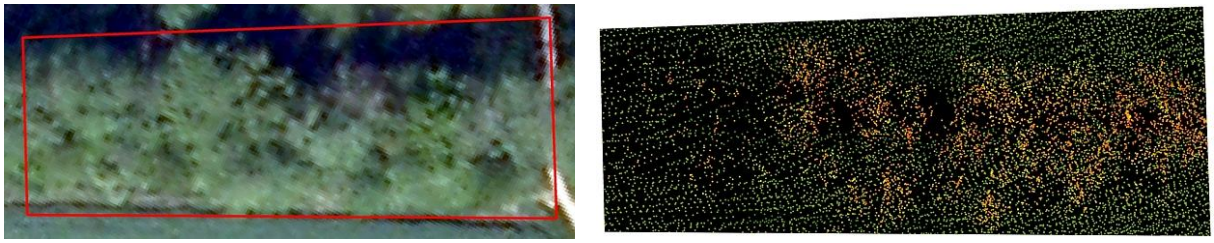

Alder belt 6

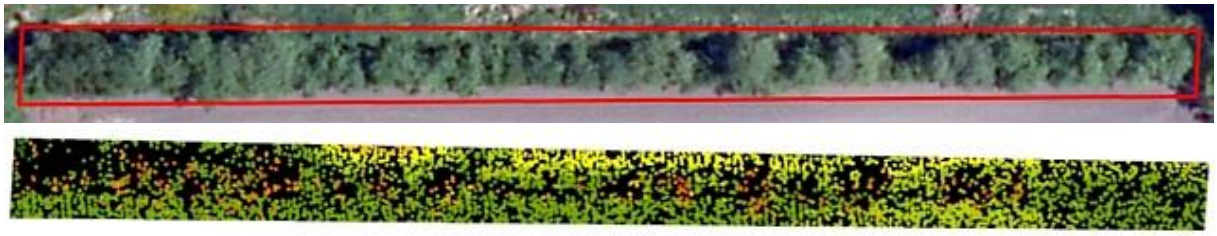

Alder belt 7

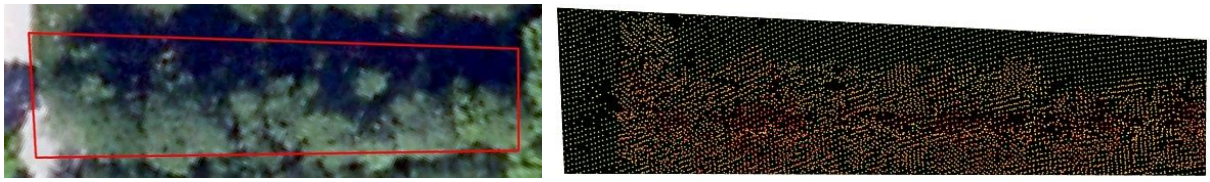

Alder belt 8

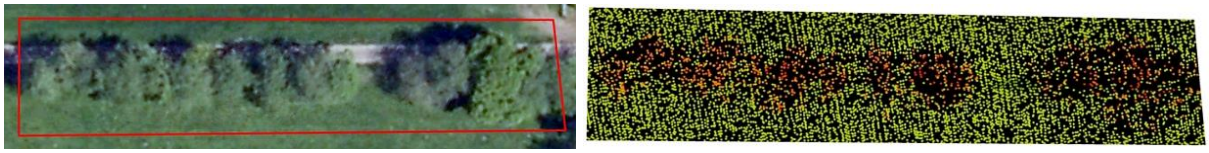

Alder belt 9

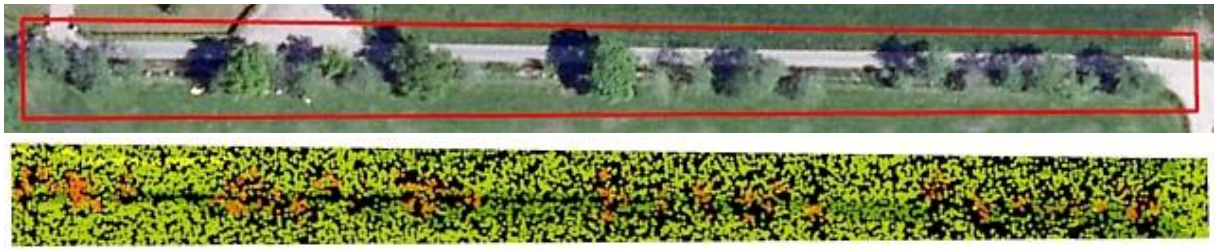

Row of trees 1

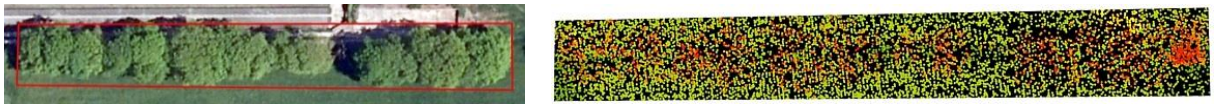

Row of trees 2

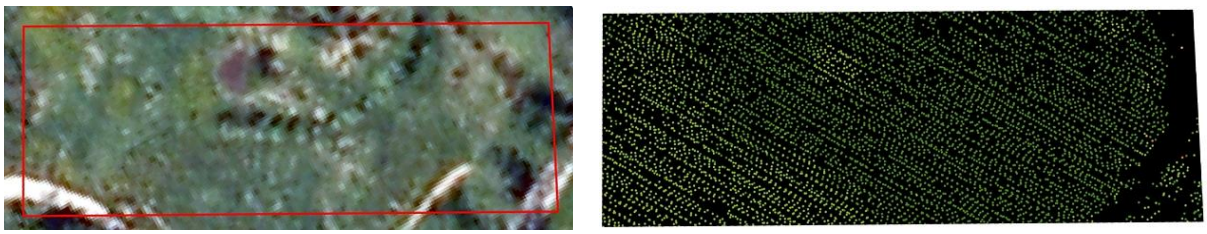

Row of trees 3

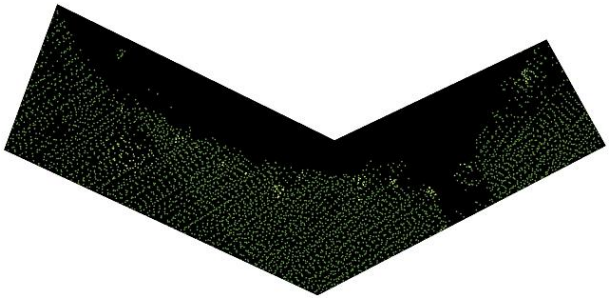

Appendix 2 Small green landscape element classification model

Pre-processing phase

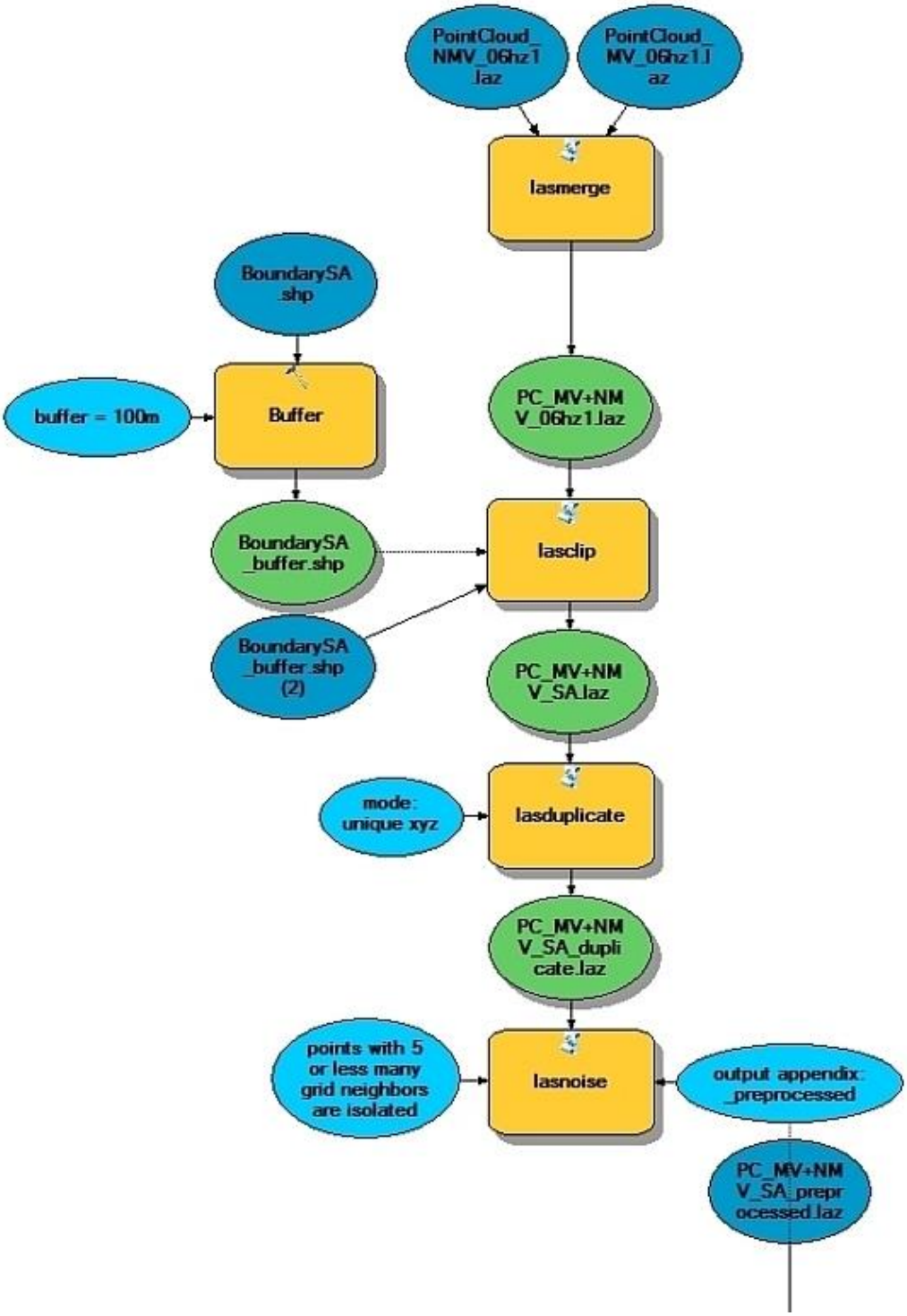

Step 1: creation of an unclassified vegetation point cloud dataset

Step 2: classification of small green landscape elements

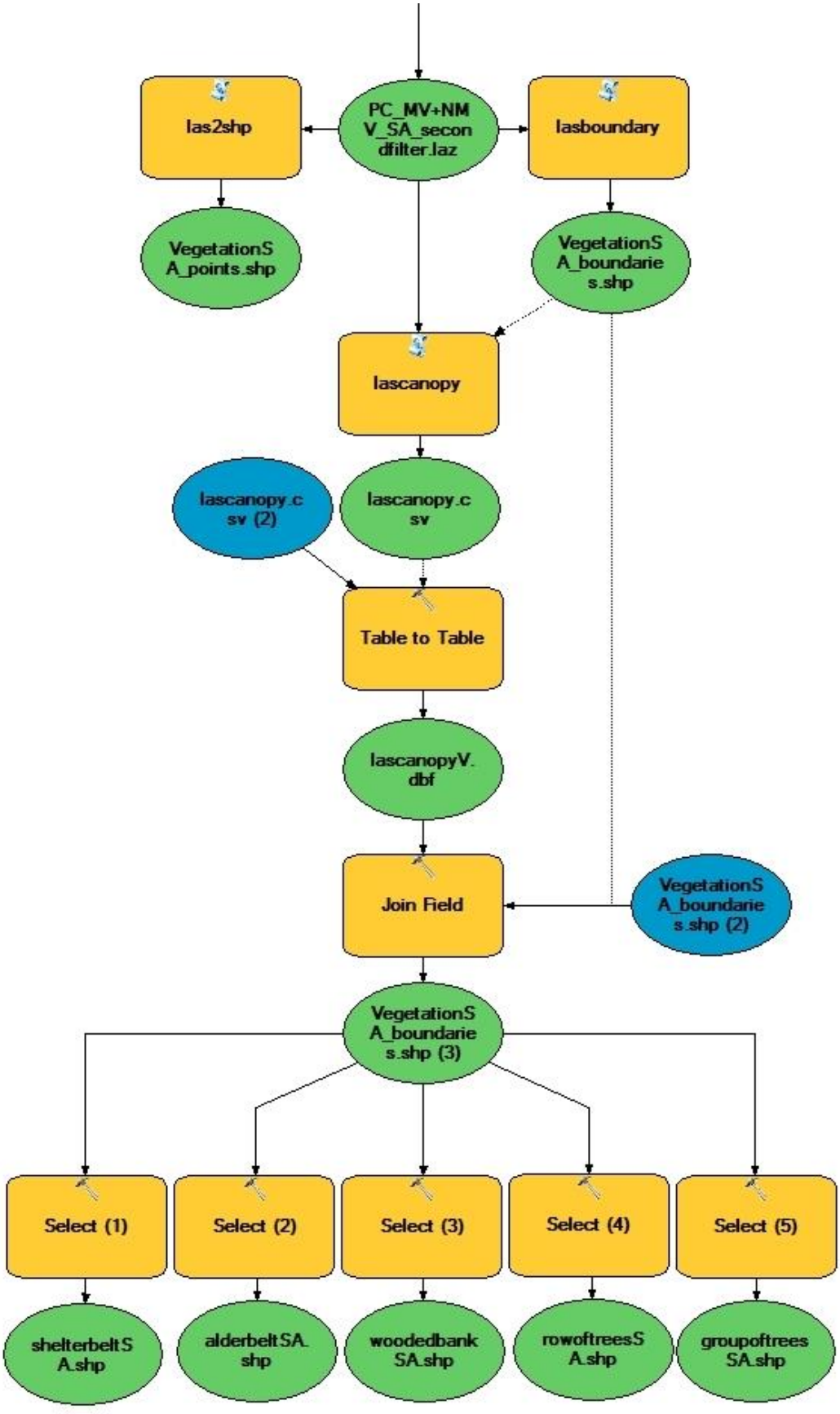

Appendix 3 Normability plots for shelterbelts and alder belts

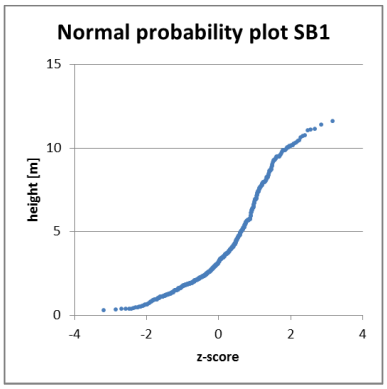

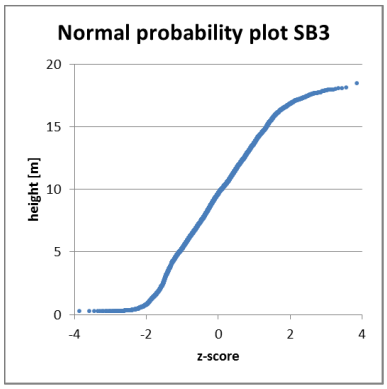

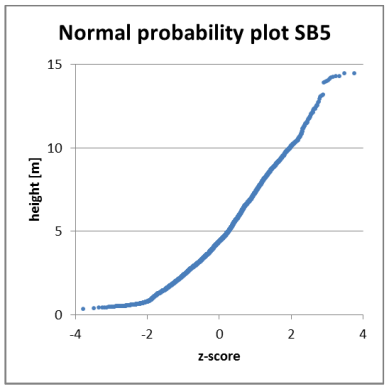

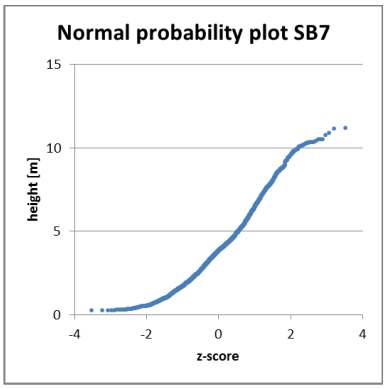

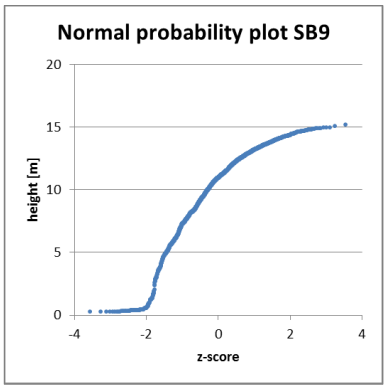

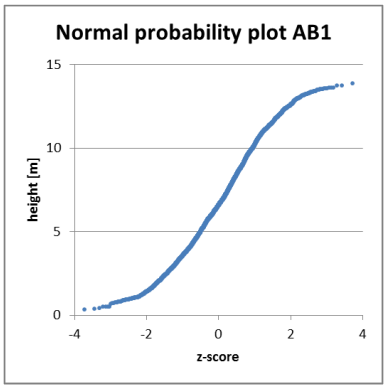

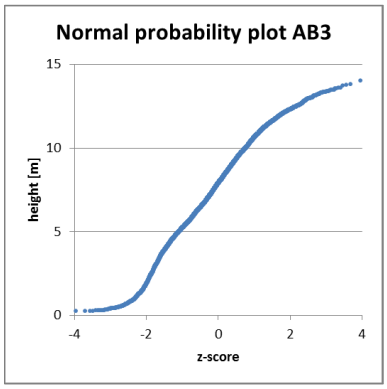

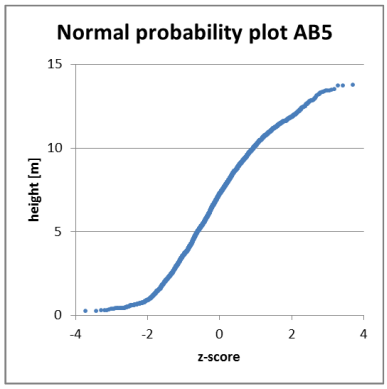

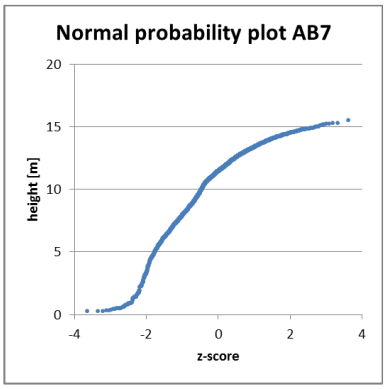

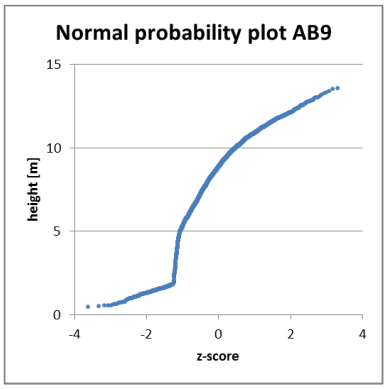

Appendix 4 Comparison of statistical results from shelterbelts and alder belts with selection criteria for small green landscape element classification